CHAPTER THREE

PSAMMITIC ROCKS (GREYWACKES)

3.1 INTRODUCTION

The term 'greywacke' here refers to immature lithic arenites possessing a significant phyllosilicate component. Such rocks are abundant throughout the New England Fold Belt. Those studied belong to the quartz-poor to quartz-intermediate lithic greywackes, of predominantly volcanic origin, described by Korsch (1977) in his Sandon Association.

Progressive contact metamorphism of the greywackes has been investigated across the aureole of the Mt Duval Adamellite. Although samples have been examined from throughout the aureole, this study concentrates on those from three major traverses (Fig. 3-1). The Mt Duval Adamellite is an elongate body with an average outcrop width of six km. The aureole is approximately 2½ km wide, within which three distinct metamorphic zones have been recognised in the greywackes. Sediments outside this aureole show effects of only very low-grade regional metamorphism. Samples from the Mt Duval aureole have been supplemented by further samples from the northeastern contact of the Uralla Granodiorite.

3.2 GEOCHEMISTRY

Analyses of ten selected greywackes are presented in Table 3.1. These analyses are very similar to the average greywacke composition calculated by Pettijohn (1975) (also shown in Table 3.1). They have relatively high Na_2O/K_2O values (greater than one), characteristic of rocks derived from a soda-rich volcanic provenance.

The major elements are plotted against distance from the contact, in Fig. 3-2. The graphs of all elements, except H, show no systematic variation with distance from the pluton, and the points are generally closely distributed around a mean. A few points lie well off the mean (circled in Fig. 3-2), but most of these values are believed to be original features inherited from the parent rocks (i.e. a high Ti content in sample C49, and low values of Fe^{2+}, Mg and Ti in sample 187 reflecting its more-felsic composition compared to the other samples). Although sample 189 is relatively high in Fe^{3+}, it has low Fe^{2+}, and total Fe is similar to

Figure 3-1: Sample locality map of greywackes from the Mt Duval Adamellite and Uralla Granodiorite contact aureoles. The general geology is based on Neilson (1971), and modified by the present author. The grid corresponds to that on the Armidale 1:100,000 topographic sheet. Sample numbers greater than 400 refer to numbers prefixed by 30 (e.g. 419 refers to 30419).

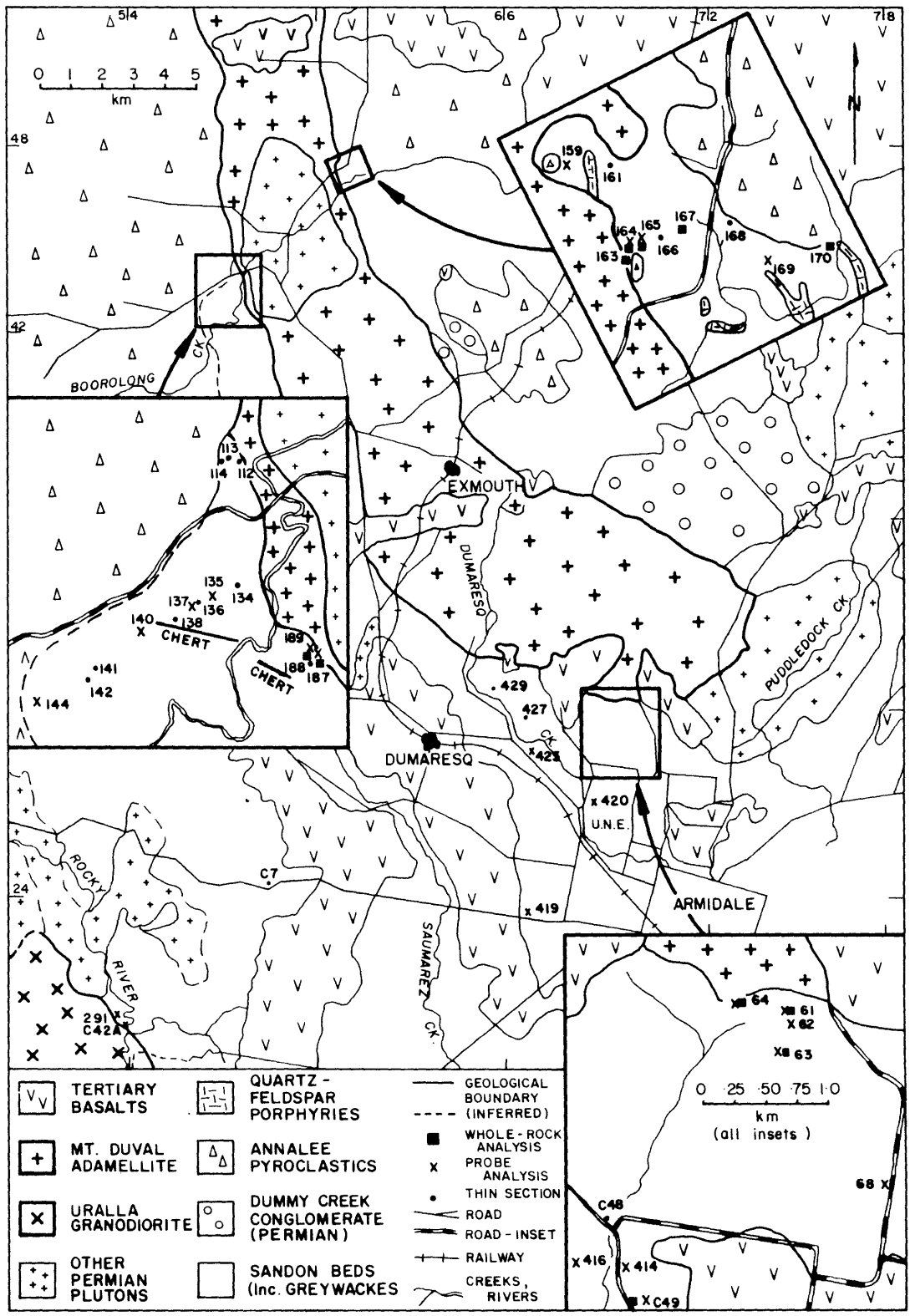
514
616
712
718
0 1 2 3 4 5
km
48
42
BOOROLONG
CK.
159
161
163
164
165
166
167
168
169
170
113
114
112
135
134
137
136
140
138
CHERT
189
188
187
141
142
144
EXMOUTH V
DUMARESQ
429
427
423
DUMARESQ CK.
PUDDLEDOCK CK.
420
U.N.E.
ARMIDALE
C7
24
ROCKY
RIVER
291
C42A
419
SAUMAREZ CK.
64
61
62
63
0 .25 .50 .75 1.0
km
(all insets)
68
C48
416
414
C49
TERTIARY BASALTS
MT. DUVAL ADAMELLITE
URALLA GRANODIORITE
OTHER PERMIAN PLUTONS
QUARTZ-FELDSPAR PORPHYRIES
ANNALEE PYROCLASTICS
DUMMY CREEK CONGLOMERATE (PERMIAN)
SANDON BEDS (Inc. GREYWACKES
GEOLOGICAL BOUNDARY
(INFERRED)
WHOLE-ROCK ANALYSIS
PROBE ANALYSIS
THIN SECTION
ROAD
ROAD-INSET
RAILWAY
CREEKS, RIVERS

TABLE 3.1. Chemical analyses of greywackes from the Mt Duval aureole

SAMPLE NO.	187	189	163	164	165	61	167	63	170	C49	PETTIJOHN (1975)
DISTANCE FROM THE CONTACT	CONTACT	30m	60m	80m	150m	150m	500m	500m	1500m	OUTSIDE AUREOLE	AVERAGE GREYWACKE
SiO_2	71.42	67.44	67.52	68.23	71.41	66.85	70.85	67.01	67.98	68.34	64.70
TiO_2	0.43	0.58	0.56	0.55	0.54	0.53	0.48	0.68	0.56	0.80	0.50
Al_2O_3	14.20	15.00	15.14	14.26	12.88	15.74	13.29	14.61	14.59	14.12	14.80
Fe_2O_3	0.74	1.90	0.71	0.68	0.86	0.88	0.64	0.94	0.88	0.51	1.50
FeO	2.28	2.31	3.30	3.70	3.17	2.91	3.22	3.75	3.58	3.50	3.90
MnO	0.06	0.08	0.06	0.07	0.07	0.05	0.08	0.08	0.08	0.07	0.10
MgO	1.04	1.48	1.68	1.68	1.42	1.59	1.54	1.98	1.84	1.81	2.20
CaO	2.34	2.38	2.54	2.61	2.03	2.16	1.97	2.66	3.02	2.50	3.10
Na_2O	4.14	4.35	3.79	3.91	3.34	4.23	3.28	4.11	3.48	3.38	3.10
K_2O	2.40	3.02	3.15	2.73	2.92	3.31	3.14	2.53	2.61	2.82	1.90
P_2O_5	0.10	0.11	0.10	0.13	0.11	0.12	0.10	0.13	0.12	0.10	-
H_2O^+	0.49	0.74	0.71	0.75	0.82	0.85	1.08	0.69	0.70	1.81	3.10
H_2O^-	0.17	0.17	0.21	0.21	0.20	0.29	0.28	0.22	0.25	0.15	
Total	99.81	99.56	99.47	99.51	99.77	99.51	99.95	99.39	99.70	99.91	99.70
Trace Elements (ppm)											
Rb	80	95	106	89	103	121	109	98	89	83	
Sr	292	366	435	351	320	453	298	386	372	363	
Y	21	17	20	22	25	26	27	27	23	42	
Zr	155	132	146	144	193	145	142	158	138	158	
Nb	9	8	9	9	10	8	9	12	12	8	
MgO/MgO+FeO	0.313	0.391	0.337	0.312	0.309	0.353	0.324	0.346	0.340	0.341	0.361

Analyses by R.H. Roberts. All analyses by X R F except Na_2O, FeO, H_2O^+ and H_2O^-, which were done by wet chemistry.

Figure 3-2: Variations in major-element chemistry with distance from the contact.

The data are taken from Table 3.1.

Samples discussed in the text are labelled.

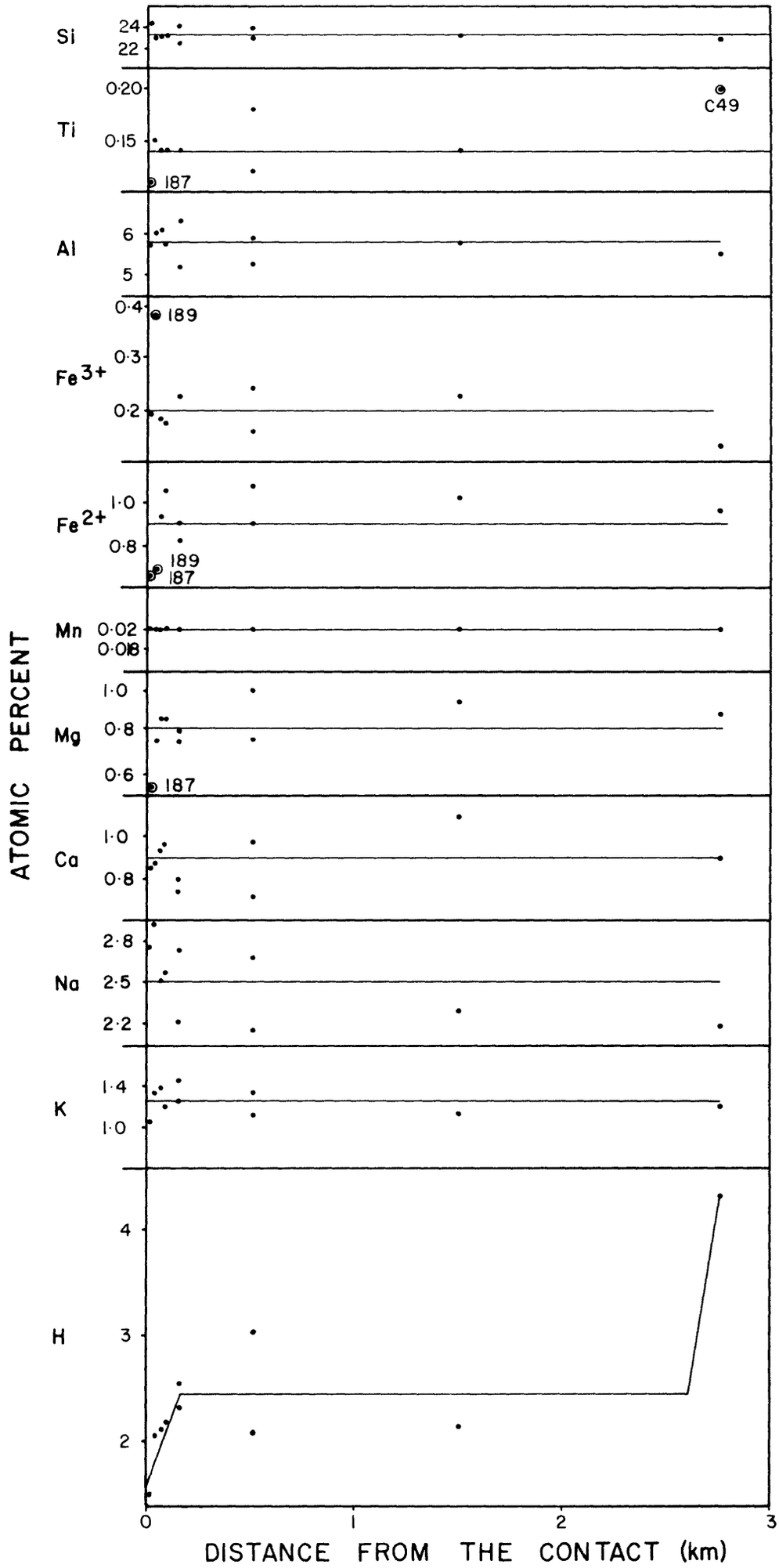
ATOMIC PERCENT
Si
24
22
Ti
0·20
0·15
C49
187
Al
6
5
Fe3+
0·4
0·3
0·2
189
Fe2+
1·0
0·8
189
187
Mn
0·02
0·018
Mg
1·0
0·8
0·6
187
Ca
1·0
0·8
Na
2·8
2·5
2·2
K
1·4
1·0
H
4
3
2
0
1
2
3
DISTANCE FROM THE CONTACT (km)

that of other samples. This is consistent with the presence of hematite (in veins and staining other minerals) within sample 189, presumably related to surface weathering. The graph of H (water content) shows two distinct decreases with increasing grade, one at the outer aureole limit (approximately 2½ km from the contact) and one at 150 metres from the contact. These decreases in water content can be related to the dehydration reactions associated with the incoming of biotite and orthopyroxene, respectively (discussed in Section 3.6).

Trace elements Rb, Sr, Y, Nb and Zr are plotted against distance from the contact in Fig. 3-3. No systematic variations with distance are seen, except for a possible decrease in Y towards the contact. One major deviation from the mean in these graphs is a high Y value for C49 (circled). This is consistent with a high percentage of sphene in this rock (which correlates with the high Ti content of sample C49, noted above), for Y preferentially concentrates into sphene (Taylor, 1966). The possible trend in Y may also correlate with a general decrease in sphene at higher grade (Section 3.4).

In summary, excluding changes in water content due to dehydration, contact metamorphism of the greywackes in the Mt Duval aureole has been isochemical.

3.3 PETROGRAPHY OUTSIDE THE AUREOLE

In hand specimen the greywackes are massive, have a clastic texture with obvious crystal and lithic fragments, and display a characteristic steel blue-grey colour when unweathered. In thin section they consist of a poorly sorted accumulation of fragments in a grain-supported texture. The abundances of fragments vary considerably, but are generally 50-60% lithic fragments, 25-35% crystal fragments, with the remainder now consisting of finer-grained phyllosilicates. Grainsize varies from siltsize to over 5 mm, but typically lies between 0.2 mm and 2 mm.

The lithic component of the greywackes consists mainly of acid to intermediate volcanic fragments. These are dominantly quartz- and feldspar-rich porphyritic types, though fragments possessing a more trachytic texture are also present. Rhyolitic volcanic fragments are less common, but are readily recognised by their distinctive spherulitic texture. These

Figure 3-3: Variations in trace-element chemistry with distance from the contact.

The data are taken from Table 3.1.

Sample C49 is discussed in the text.

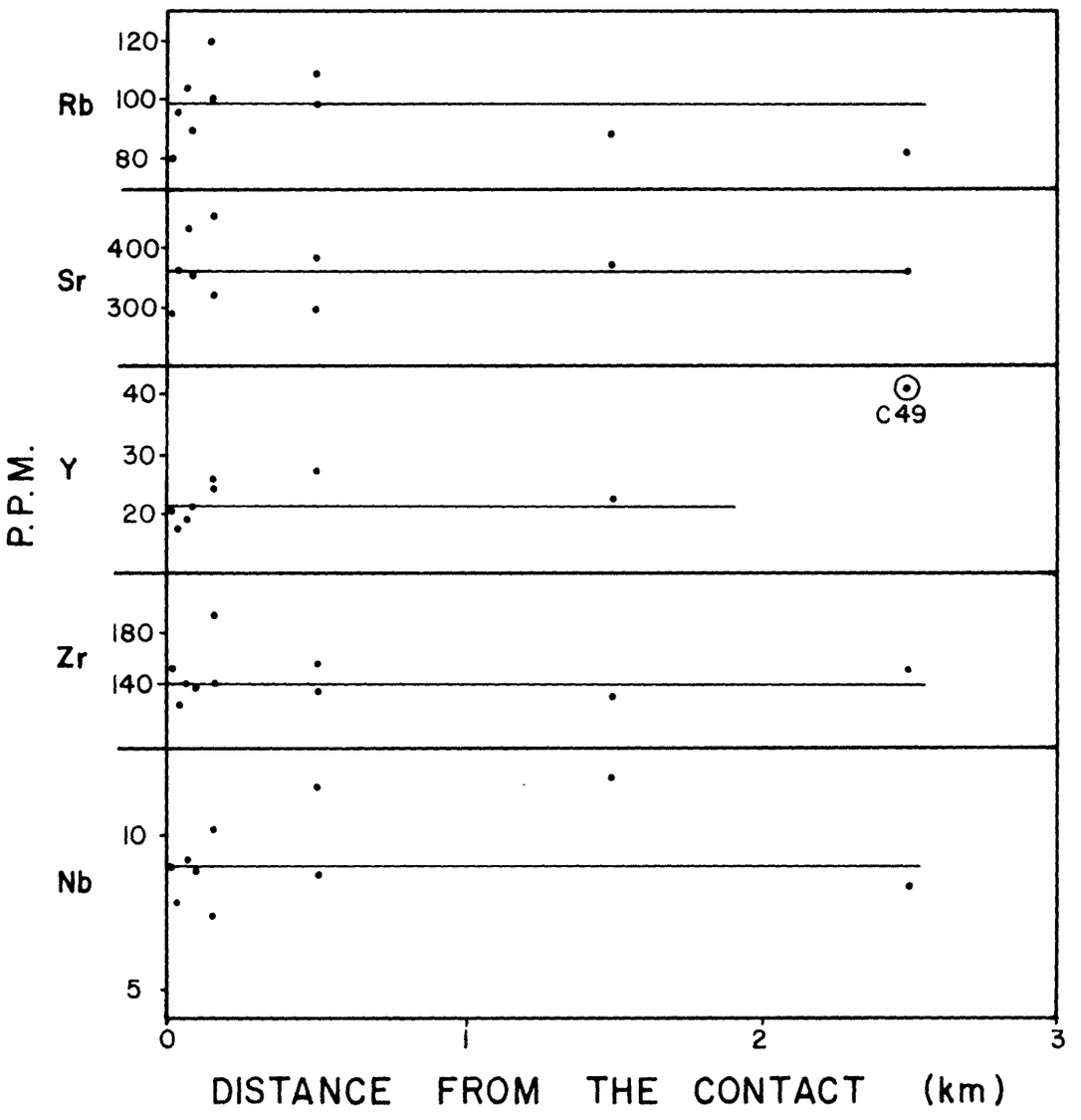
120
100
80
Rb
400
300
Sr
40
30
20
Y
C49
180
140
Zr
10
5
Nb
P.P.M.
0
1
2
3
DISTANCE FROM THE CONTACT (km)

fragments consist mainly of K-rich sanidines, though Na content can range high enough for some feldspar to be classified as anorthoclase (Ab > 63). Other igneous fragments include basaltic, doleritic and granophyric types. Sedimentary rock fragments usually form only 3-4% of these rocks and include chert, siltstone and argillite.

Quartz and feldspar comprise over 40% of the mineral fragments. Several compositionally different feldspars are present. Well twinned and zoned plagioclases have core compositions of andesine to oligoclase (Ab 67 to 72) with more-sodic rims ranging up to Ab 90. Subidiomorphic crystals of albite (Ab > 90), K-feldspar (Or > 90) and to a lesser extent anorthoclase (Ab > 63) are present, and characteristically lack the obvious twinning of the more-calcic plagioclase. Typical feldspar analyses are given in Table 3.2.

The minor components consist of detrital biotite, amphibole, epidote, opaque oxides (predominantly ilmenite), plus rare pyroxene, muscovite, and accessory zircon, apatite and rutile. The amphiboles commonly occur as coarse subhedral grains, and are generally actinolitic in composition (two analyses from sample C49 are shown in Table 3.2). The biotites also occur as coarse grains, are typically kinked, and are characterised by patchy red-brown alteration. Analyses of biotites showing various degrees of alteration are listed in Table 3.2 along with estimates of the original biotite composition and possible alteration product. The alteration product is possibly a type of vermiculite. The degree of biotite alteration is not related to the degree of surface weathering and appears to be the result of very low-grade regional metamorphism (see below). Epidote was found in all samples as discrete coarse grains, and as finer-grained aggregates associated with sericitization of plagioclase. Both types of epidote are relatively Fe-rich (Table 3.2).

The phyllosilicate component is composed mostly of green chlorite with characteristic Berlin blue interference colour. It commonly occurs as fine-grained clusters, often within a rectangular outline, or as elongate lenses between adjacent fragments, suggesting that it developed by pseudomorphous replacement of original mineral or lithic fragments. Very fine-grained chlorite also occurs in thin fractures cutting across fragments and as thin selvedges along grain margins. The chlorites have uniform chemical composition regardless of their textural occurrence, and two typical

TABLE 3.2. Representative microprobe analyses of minerals in greywackes outside the Mt Duval aureole

	FELDSPARS				AMPHIBOLES		EPIDOTE		SERICITE	CHLORITE				BIOTITE ALTERATION[d]				
Sample No.	Plag Core 30419	Plag Rim 30419	Anorth 30441	K-f 30419	Act C49	Act C49	Detrital 30441	Plag[a] Alt C49	Plag[a] Alt C49	Matrix C49	Amph[b] Alt C49	Altered[c] 30420	Altered[c] 30419	Calc Original Biotite	30423	30420	C49	Calc Alt Product
SiO_2	60.47	65.44	67.63	65.51	52.25	54.94	38.00	37.15	47.48	25.89	26.20	29.45	33.86	N	33.85	33.40	29.21	N
TiO_2	-	0.26	-	-	0.45	0.20	-	-	0.12	-	0.07	-	0.23	O	4.52	3.28	1.41	O
Al_2O_3	24.72	20.29	19.96	18.22	1.79	0.23	22.87	23.44	36.71	20.29	20.15	17.50	17.19	T	16.34	15.60	17.72	T
Fe_2O_3					0.30*	0.23*	14.68**	12.14**						C				C
FeO	-	1.82	-	-	13.08	10.94	-	0.43	0.23	29.11	28.85	26.95	24.92	A	21.28	25.19	26.73	A
MnO	-	-	-	-	0.57	0.34	0.44	0.22	-	0.54	0.45	0.48	0.31	L	0.20	0.30	0.48	L
MgO	-	-	-	-	15.58	17.41	-	0.86	0.23	11.97	11.75	12.55	11.37	C	7.59	10.88	12.00	C
CaO	6.83	1.66	0.15	-	11.56	12.31	23.36	21.10	0.25	-	0.11	0.32	0.52	U	-	0.20	0.27	U
Na_2O	8.19	10.09	9.35	0.90	0.47	0.21	-	-	0.80	0.12	0.20	-	0.27	L	-	-	-	L
K_2O	0.38	0.35	2.83	15.55	0.23	-	-	-	10.21	0.06	-	-	0.34	A	6.92	4.62	2.12	A
														T				T
														E				E
														D				D
Total	100.59	99.91	99.92	100.18	96.28	96.81	99.35	95.34	96.04	87.98	87.78	87.25	89.01					
Structural formulae																		
No. of oxygens	32	32	32	32	23	23	25	25	22	28	28	28	28	22	22	22	22	22
Si	10.741	11.605	11.918	12.046	7.688	7.916	5.997	6.035	6.212	5.557	5.623	6.255	6.893	5.80	5.430	5.248	4.790	4.50
Al^{IV}	5.179	4.243	4.148	3.951	0.311	0.039	0.003	-	1.788	2.443	2.377	1.745	1.107	2.20	2.570	2.752	3.210	3.50
Al^{VI}	-	-	-	-	-	-	4.252	4.489	3.873	2.693	2.723	2.639	3.020	0.60	0.525	0.139	0.217	-
Ti	-	0.035	-	-	0.050	0.022	-	-	0.012	-	0.011	-	0.035	0.70	0.546	0.388	0.174	-
Fe^{3+}					0.034	0.025	1.744	1.484										
Fe^{2+}	-	0.270	-	-	1.609	1.318	-	0.058	0.025	5.225	5.178	4.787	4.243	2.60	2.856	3.310	3.666	4.00
Mn	-	-	-	-	0.071	0.041	0.059	0.030	-	0.098	0.082	0.086	0.054	-	0.027	0.040	0.067	0.06
Mg	-	-	-	-	3.416	3.738	-	0.208	0.046	3.829	3.758	3.972	3.449	1.75	1.815	2.548	2.933	3.40
Ca	1.300	0.315	0.028	-	1.823	1.901	3.950	3.673	0.035	-	0.025	0.073	0.113	-	-	0.034	0.047	-
Na	2.820	3.469	3.195	0.321	0.134	0.059	-	-	0.204	0.050	0.083	-	0.107	-	-	-	-	-
K	0.085	0.079	0.636	3.649	0.043	-	-	-	1.704	0.016	-	-	0.088	1.80	1.417	0.926	0.444	-
Total cations	20.125	20.016	19.925	19.967	15.179	15.059	16.005	15.977	13.899	19.912	19.861	19.557	19.109	15.45	15.186	15.384	15.547	15.46
Or	2.03	2.05	16.49	91.92														
Ab	67.06	89.79	82.78	8.08														
An	30.92	8.16	0.73	-														
Mg/Mg+Fe					0.680	0.739				0.423	0.421			0.402	0.389	0.435	0.444	0.459

* Fe_2O_3 calculated by method of Papike *et al.* (1974)

** Fe_2O_3 based on 16 cations

Plag = plagioclase, Anorth = anorthoclase, K-f = K-feldspar, Act = actinolite, Alt = alteration, Calc = calculated.

a: associated with sericitization of plagioclase, b: occurs within precursor amphibole, c: altered chlorite - alteration is more intense in sample 30419 than in 30420.

d: biotite alteration increases in intensity in the direction of the arrow - structural formulae for possible compositions of the unaltered biotite and the alteration product have been calculated from various degrees of alteration in the biotites.

analyses are shown in Table 3.2. Red-brown sphene is often closely associated with the chlorite, while a very fine-grained mixture of chlorite and sphene, identified with the electron microprobe, is present as a grey-brownish material ubiquitously surrounding fragment boundaries. Modally, the chlorite and coarser sphene together occupy approximately 10-12% by volume, and the finer aggregates nearly 5%. The chlorite within these rocks appears to have been readily altered by surface weathering, developing a brown to red-brown colouration. Analyses of two altered chlorites are presented in Table 3.2 (the chlorite from sample 30419 is more altered than that from sample 30420). The alteration product appears to be iron-rich vermiculite. These observations are in agreement with those of Brown (1967), who pointed out that this brownish alteration should not be confused with biotite. White mica is present only as rare detrital grains and in minor amounts as sericitic alteration of plagioclase (a representative analysis of sericite is shown in Table 3.2).

Modal data on samples representative of greywackes outside the aureole are presented in Table 3.3, along with modal analyses taken throughout the aureole.

3.4 PETROGRAPHY OF THE CONTACT METAMORPHOSED ROCKS

Three metamorphic zones, distinguished by both texture and mineral assemblage, have been mapped parallel to the pluton perimeter. These are (with distance from the contact given in brackets)

I) Blastopsammitic Biotite Zone (2½ km - 500 m);
II) Transitional Biotite Zone (500 m - 150 m);
III) Biotite+Orthopyroxene Zone (150 m - Contact).

3.4.1 Blastopsammitic Biotite Zone

Contact metamorphism is first evidenced in greywackes by the appearance of biotite. The biotite isograd is sharp, and in the Mt Duval Adamellite aureole is consistently located approximately 2½ km from the pluton contact.

In hand specimen the rock takes on a characteristic grey-black colour, in contrast to its bluer appearance outside the aureole. However,

TABLE 3.3. Modes of greywackes from the Mt Duval aureole showing variation with increasing grade of contact metamorphism

SAMPLE	DISTANCE FROM THE CONTACT		MINERAL GRAINS							LITHIC FRAGMENTS				PHYLLOSILICATES				DEGREE*** OF RECONSTITUTION
			QUARTZ	K-FELD	PLAG	OPAQUES	EXTRAS	OPX	TOTAL	VOLC	PLUT	SED	TOTAL	FINE-GR CHL+SPH	CHLORITE	BIOTITE	TOTAL	
OUTSIDE THE AUREOLE																		
30420			15.0	4.0	7.0	0.6	1.2†		27.8	49.1#	0.8	2.0	51.9	8.3	12.0		20.3	
C7			16.2	7.1	17.1	1.0	2.8†		44.8	35.0#	0.2	2.1	37.3	5.6	11.9		17.9	
C28			12.5	5.0	10.0	3.0	5.5†		36.0	48.5#	-	1.7	50.2	5.3	8.5		13.8	
C49			13.0	1.5	7.5	0.8	1.4†		24.2	47.8#	0.2	17.6	64.4	4.8	5.6		10.4	
BLASTOPSAMMITIC BIOTITE ZONE																		
30423	2100m		8.3	2.0	13.0	2.7			26.0	45.3		0.7	46.0	**	-	28.0	28.0	
30427	1500m		17.3	1.8	6.7	0.2			26.0	51.1		0.4	51.5		0.5[X]	22.0	22.5	
30429	1000m		10.5	0.8	19.2	0.5			31.0	50.0		0.5	50.5		1.8[X]	16.0	18.5	
TRANSITIONAL BIOTITE ZONE																		
167	500m	*RELICT	18.3	4.0	11.5	0.2			34.0	17.2		3.9	21.1		0.7[X]	14.5	15.2	44.9%
		MET	3.9		25.8				29.7									
63	500m	RELICT	13.0	0.5	13.0	0.2			26.7	17.5		1.5	19.0		-	24.2	24.2	54.1%
		MET	4.3		25.8				30.1									
166	300m	RELICT	14.4	1.6	7.2	0.4			23.6	13.0		1.8	14.8		4.4[X]	15.6	20.0	61.6%
		MET	7.4		34.2				41.6									
62	250m	RELICT	13.0	3.0	9.0	-			25.0	4.3		4.9	9.2		0.5[X]	21.7	22.2	65.8%
		MET	9.3		28.9	1.2	4.2[≠]		43.6									
ORTHOPYROXENE+ BIOTITE ZONE																		
165	150m	RELICT	10.0	1.0	3.0	-			14.0									
		MET	5.2	9.8	45.4	0.2		9.0	69.6						0.6[X]	15.8	16.4	86.0%
61	150m	RELICT	-	-	-	-			-									
		MET	26.4	15.6	39.4	-		1.0	82.5						-	17.5	17.5	100.0%
163	60m	RELICT	0.2	-	1.8	-			2.0									
		MET	19.8	19.6	37.6	0.2		6.8	84.0						1.0[X]	13.0	14.0	98.0%
161	CONTACT	RELICT	4.0	-	1.6	-			5.6									
		MET	17.2	19.8	36.4	0.2		5.0	78.8						1.6[X]	14.2	15.6	94.4%
291	CONTACT	RELICT	-	-	-	-												
		MET	34.7	18.3	26.4	0.8		9.9	90.1						-	9.9	9.9	100.0%

* Relict and metamorphic grains are recognised in the inner zones.
** Fine-grained sphene is present in the biotite zones, though its modal content is difficult to determine amongst biotite. X Retrograde chlorite.
† Possible extras include epidote, altered relict biotite, amphibole, minor pyroxene and accessories. ≠: cummingtonite, # Volcanic fragments include rhyolitic fragments possessing a spherulitic texture. *** Refers to the percentage of original components converted to metamorphic minerals by contact metamorphism.

All samples are located in Fig.3-1 except C28. C28 occurs at GR 285-280 on the Torryburn 1:25,000 topographic sheet.
Abbreviations: K-FELD = K-feldspar, OPX = orthopyroxene, VOLC = volcanic, PLUT = plutonic, SED = sedimentary, FINE-GR CHL+SPH = fine-grained chlorite+sphene
Anorthoclase is included with the K-feldspar. However, anorthoclase that has been insensitive to the Na-cobaltinitrite stain may have been counted with plagioclase.

besides colour, the rock's macroscopic appearance is hardly altered. Microscopically, the metagreywacke has a texture identical to that outside the aureole (Plates 3-1A and 3-2A).

Biotite occupies between 20% and 25% by volume of the rock. It forms as small indistinct grains which mimic the textural occurrence of the pre-existing chlorite plus sphene, occurring in interstitial clusters and along grain boundaries and fractures. The lowest-grade biotite has a green to yellow-green colour, but brown biotite rapidly predominates with increasing grade in the blastopsammitic biotite zone. The biotite isograd marks the immediate disappearance of chlorite, and a sharp decrease in sphene, which persists within the biotite zones as fine-grained brown interstitial material.

This boundary coincides with the loss of several minor phases, including epidote and amphibole. Similarly, altered relict biotite grains (described in Section 3.3), although still present in the outer part of the blastopsammitic biotite zone, are partially replaced by newly crystallising biotite, and completely replaced at higher grade. The feldspars show little change, though the abundances of K-feldspar, anorthoclase and albite have decreased. Rhyolitic fragments possessing spherulitic texture, which were prominent outside the aureole, are not obvious on the high-grade side of the biotite isograd. Sedimentary fragments are still discernible, but the original dark argillaceous clasts now contain fine-grained biotite.

With increasing grade across the zone, only minor changes occur to the petrographic features described above. Biotite continues to coarsen and become a darker brown colour, and in the inner parts of this zone develops a poor decussate texture. The relict psammitic texture remains obvious in these rocks until approximately 500m from the contact. This is taken as the inner limit of the blastopsammitic biotite zone.

3.4.2 Transitional Biotite Zone

At 500m from the contact, fine-grained lithic fragments (predominantly volcanic) are texturally modified by grain growth, presumably initiated by the increase in temperature. This has caused the original texture within the volcanic fragments, dominated by feldspar laths, to be converted to a fine-grained granoblastic-polygonal texture. The general outline

Plate 3-1: Textural variation in the greywackes with increasing grade of contact metamorphism. Photographs taken under crossed polars.

These photographs are identical to those in Plate 3-2, except that the latter were photographed under plane-polarized light. The width of each photograph covers 3.60 mm.

A: Blastopsammitic Biotite Zone (Sample 170).

The greywacke possesses a clastic texture of lithic and crystal fragments identical to those outside the aureole (more obvious in Plate 3-2A). Twinning can be seen in some plagioclase grains. Quartz fragments are white. A large volcanic lithic fragment is present in the upper middle part of the photograph. Fine-grained biotite occurring between the fragments is not discernible.

B: Transitional Biotite Zone (Sample 166).

Lithic fragments are texturally modified to a fine-grained granoblastic-polygonal texture. A large lithic fragment is shown in the bottom right corner of the photograph. Relict quartz grains are replaced by polygonal aggregates of strain-free quartz (e.g. bottom left corner).

C: Inner Boundary of the Transitional Biotite Zone (Sample 165)

The rock has a higher degree of reconstitution (cf. photograph B). The texture is becoming more granoblastic and lithic fragments are hard to distinguish.

D: Biotite + Orthopyroxene Zone (Sample 163)

Almost complete loss of the original clastic texture. Grainsize is considerably coarser, and a granoblastic-polygonal texture is well developed. Biotite occurs as randomly orientated coarse flakes. (More apparent in Plate 3-2D).

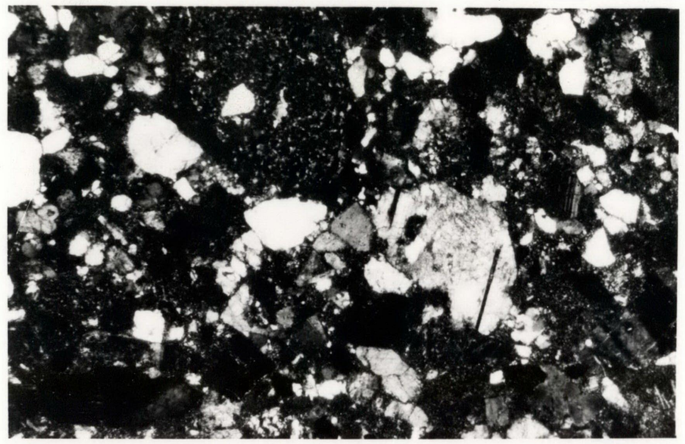

A

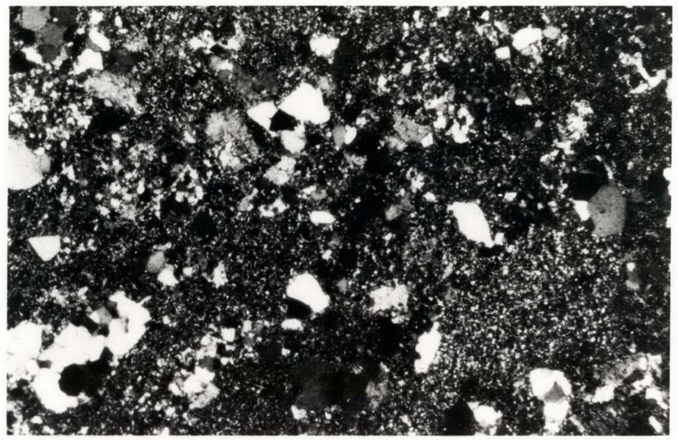

B

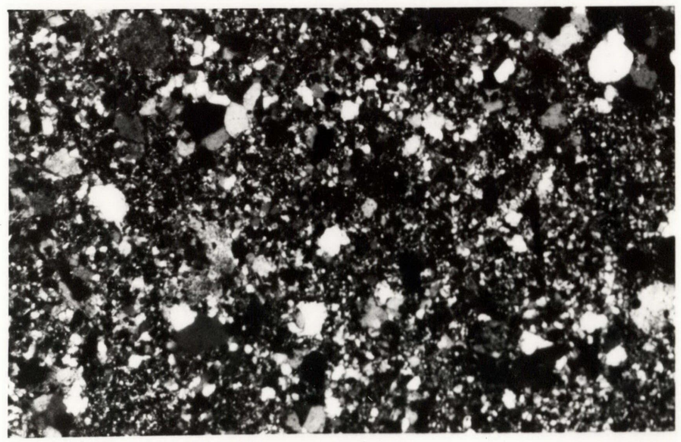

C

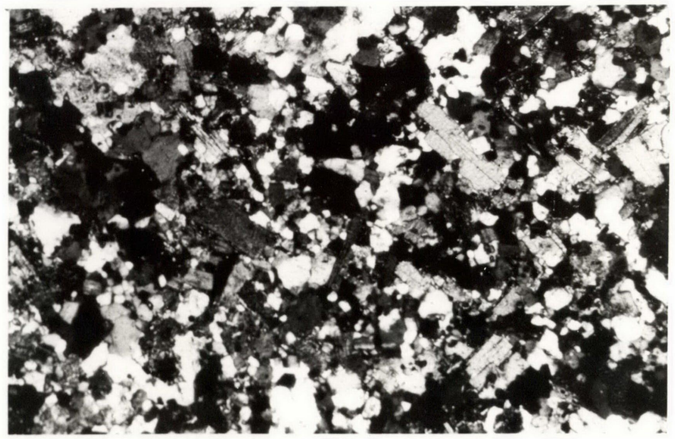

D

Plate 3-2: Textural variation in the greywackes with increasing grade of contact metamorphism. Photographs taken under plane-polarized light.

These photographs are identical to those in Plate 3-1, except that the latter were photographed under crossed polars. The width of each photograph covers 3.60 mm.

A: Blastopsammitic Biotite Zone (Sample 170)

The clastic texture of the greywacke is prominent. Dark patches between fragments and along grain boundaries consist predominantly of small indistinct grains of biotite.

B: Transitional Biotite Zone (Sample 166)

Lithic fragments are poorly distinguished. However, the outlines of crystal fragments are quite distinct. Small patches of biotite are evident between the fragments.

C: Inner Boundary of the Transitional Biotite Zone (Sample 165)

The texture is becoming more granoblastic and lithic fragments are hard to distinguish. Biotite is coarser-grained, more distinct, and is less confined to small clusters.

D: Biotite + Orthopyroxene Zone (Sample 163)

Coarse randomly orientated biotite flakes occur within a felsic assemblage possessing a granoblastic-polygonal texture.

A

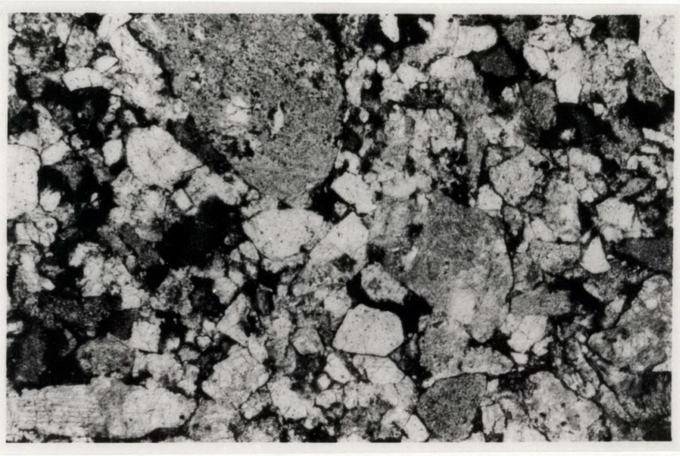

B

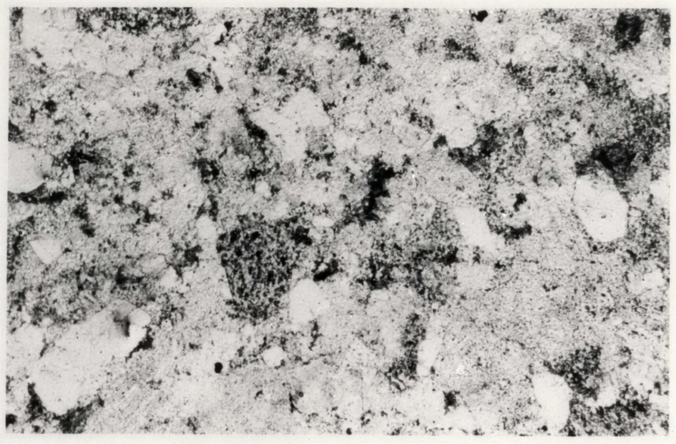

C

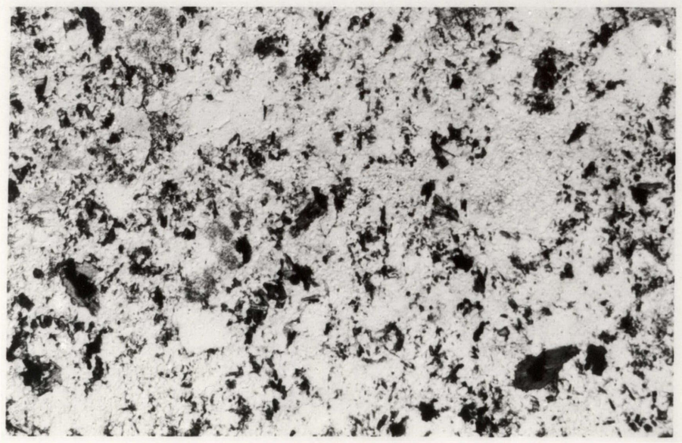

D

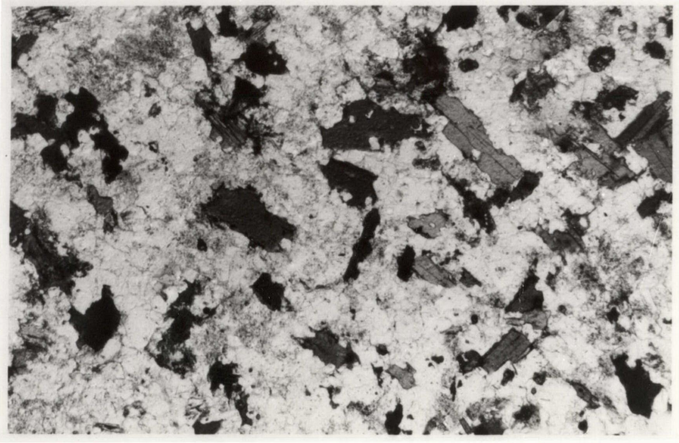

of the fragments, though, is still quite discernible, and is emphasised by the presence of decussate biotite around the fragments.

The crystal fragments also show evidence of textural adjustment. Relict quartz grains are replaced by polygonal aggregates of fine-grained strain-free quartz, and fine-grained metamorphic plagioclase has developed on the grain boundaries of relict plagioclase. These are both effects of primary recrystallisation, as defined by Wilson (1973). Primary recrystallisation also occurs in the phenocrysts of lithic fragments.

The resulting texture (Plates 3-1B and 3-2B) is quite distinct from that of the blastopsammitic zone. The textural change is witnessed in hand specimen by a more-equigranular appearance, with individual fragments becoming increasingly difficult to distinguish. The rocks have a hornfelsic texture. The degree of reconstitution increases toward the inner part of this zone as depicted by the modes of Table 3.3, and shown in Plates 3-1C and 3-2C.

3.4.3 Biotite+Orthopyroxene Zone

This zone begins around 150m from the contact and is defined by the appearance of orthopyroxene, and complete loss of the original clastic texture, except for a few remaining cores of relict plagioclase. The presence of orthopyroxene, often up to 10% by volume of the rock, is accompanied by a major increase in K-feldspar (from 2-3% to 18-19%) and a major decrease in biotite (from around 25% down to as low as 10%). Plagioclase (Ab 70) is still prevalent, but grains of albite and anorthoclase are absent. Thus, the high-grade metamorphic assemblage comprises quartz, plagioclase, K-feldspar, biotite, orthopyroxene and ilmenite. Modes for rocks within this zone are given in Table 3.3. The incoming of orthopyroxene does not, though, define a sharp boundary, as rocks lacking orthopyroxene occur within this zone. This is a compositional effect (discussed in Section 3.6).

Grainsize has coarsened considerably from around 0.01mm in the transitional zone to between 0.1mm and 0.5mm or greater. A general granoblastic-polygonal texture is developed (Plates 3-1D and 3-2D), but this is commonly interrupted by very coarse irregularly shaped grains. These coarser grains are the result of exceptional or exaggerated grain growth (Wilson, 1973), related to secondary recrystallisation. This is best

shown by K-feldspar, which forms large porphyroblasts of ragged outline containing abundant inclusions of quartz and plagioclase. Quartz also displays this feature, but to a lesser extent. Biotite no longer occurs in clusters, but as coarse, darkly coloured grains (X=straw yellow; Y=Z=red brown). In contrast, the newly formed plagioclase remains relatively fine grained and subidioblastic. Aggregates of such grains often occur around relicts of detrital plagioclase. The orthopyroxene and ilmenite are present as smaller discrete grains throughout the rock. Much of the orthopyroxene is commonly altered to retrograde amphibole (see Section 3.5.7).

These changes in mineralogy and texture are well expressed in hand specimen. Firstly, the rock takes on a lighter grey colour, compared to the grey-black colour of the outer and transitional zones. This change is attributed to the general decrease in biotite. Secondly, the increase in grainsize permits macroscopic identification of the minerals.

One exceptional outcrop (sample C42A) requires further discussion. It occurs on the northeastern edge of the Uralla Granodiorite, and displays banding that parallels the igneous contact. The banding consists of dark-brown layers of predominantly decussate biotite, and felsic layers of coarse interlocking quartz, K-feldspar, orthopyroxene, lesser plagioclase, and occasional biotite. Much of the orthopyroxene is associated with patches of fibrous cummingtonite. Boundaries between these layers are gradational. This mineralogy is consistent with the high-grade biotite + orthopyroxene zone assemblage of the greywackes. The banding could be relict bedding, but sedimentary bedding is rarely noted in the greywackes. Alternatively, the layering could have formed by metamorphic segregation, perhaps in response to stress propagated by emplacement of the pluton. If so, heating must have continued after the release of the stress, to allow formation of the decussate granoblastic texture.

3.5 MINERAL CHEMISTRY

3.5.1 Introduction

This section describes the variation in mineral chemistry throughout the aureole. Further discussion of the changes in mineral chemistry in relation to the metamorphic reactions is given in Section 3.6.

3.5.2 Feldspar

Relict feldspars within the contact-metamorphosed greywackes are identical in composition to those found in greywackes outside the aureole (Table 3.2). Newly formed plagioclase in the transitional biotite and biotite-orthopyroxene zones has an oligoclase-andesine composition (around Ab 79), and appears to increase slightly in An content with increasing grade.

3.5.3 Biotite

Biotite analyses from throughout the aureole are listed in Table 3.4, and several elements of the biotite chemistry are plotted against distance from the contact in Fig. 3-4. Fig. 3-4A shows the composition of the tetrahedral layer to be relatively constant with increasing grade. In contrast, Figs. 3-4B→F show the octahedral layer to have a marked decrease in Al^{VI} with increasing grade, which appears to be compensated by an increase in both Ti and Mg. Fe and Mn trends are less distinct, but these elements appear to decrease near the contact. As the oxidation states of Fe are not measurable on the electron microprobe, total Fe is shown as Fe^{2+}. Owing to the fine grainsize of the hornfelses, only coarser high-grade samples gave useable biotite separates for Fe^{3+} determination by wet-chemical analysis. No trends, for either Fe^{2+} or Fe^{3+} separately, could be substantiated from these limited results. All graphs in Fig. 3-4 exhibit a significant scatter of biotite compositions at any given distance from the contact. This chemical variation in the biotites occurs even between analyses from the same thin section, and thus reflects variations in host-rock composition over distances of less than a few millimetres. Therefore, the biotite analyses in Fig. 3-4 show the effects of both an original variation in the greywackes and a grade-related variation associated with the contact metamorphism.

The biotite of this study has a relatively constant tetrahedral layer composition with increasing grade (noted above). Therefore, as described by Dahl (1969), the lateral dimension of the tetrahedral layer should tend to be constant. Dahl (1969) and Dallmeyer (1974) have stated that, to prevent structural mismatch, the tetrahedral and octahedral layers in biotite must have the same lateral dimensions. Hence, substitutions in the octahedral layer should occur in such a way that the layer's lateral dimension is unchanged (i.e. if it is to remain equal to the uniform

Figure 3-4: Biotite mineral chemistry versus distance from the contact of the Mt Duval Adamellite.

Symbols: ● Brown Biotite

●(P) Pale-brown Biotite

× Green Biotite

Sum Y = Total number of ions in the octahedral layer

Sum Z = Total number of ions in the tetrahedral layer

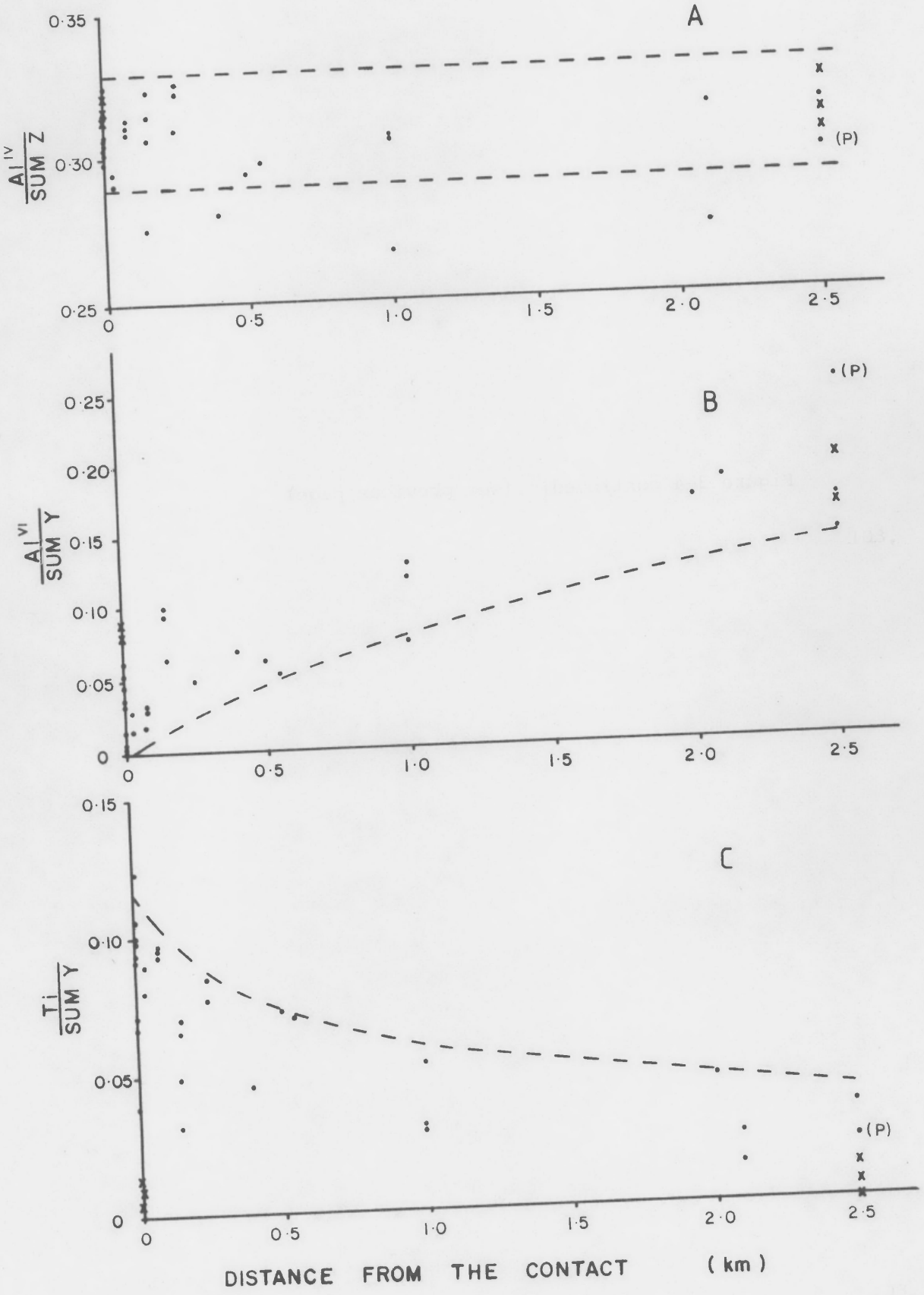
A
B
C
$\frac{Al^{IV}}{SUM\ Z}$
$\frac{Al^{VI}}{SUM\ Y}$
$\frac{Ti}{SUM\ Y}$
0·35
0·30
0·25
0·20
0·15
0·10
0·05
0
0·5
1·0
1·5
2·0
2·5
(P)
DISTANCE FROM THE CONTACT (km)

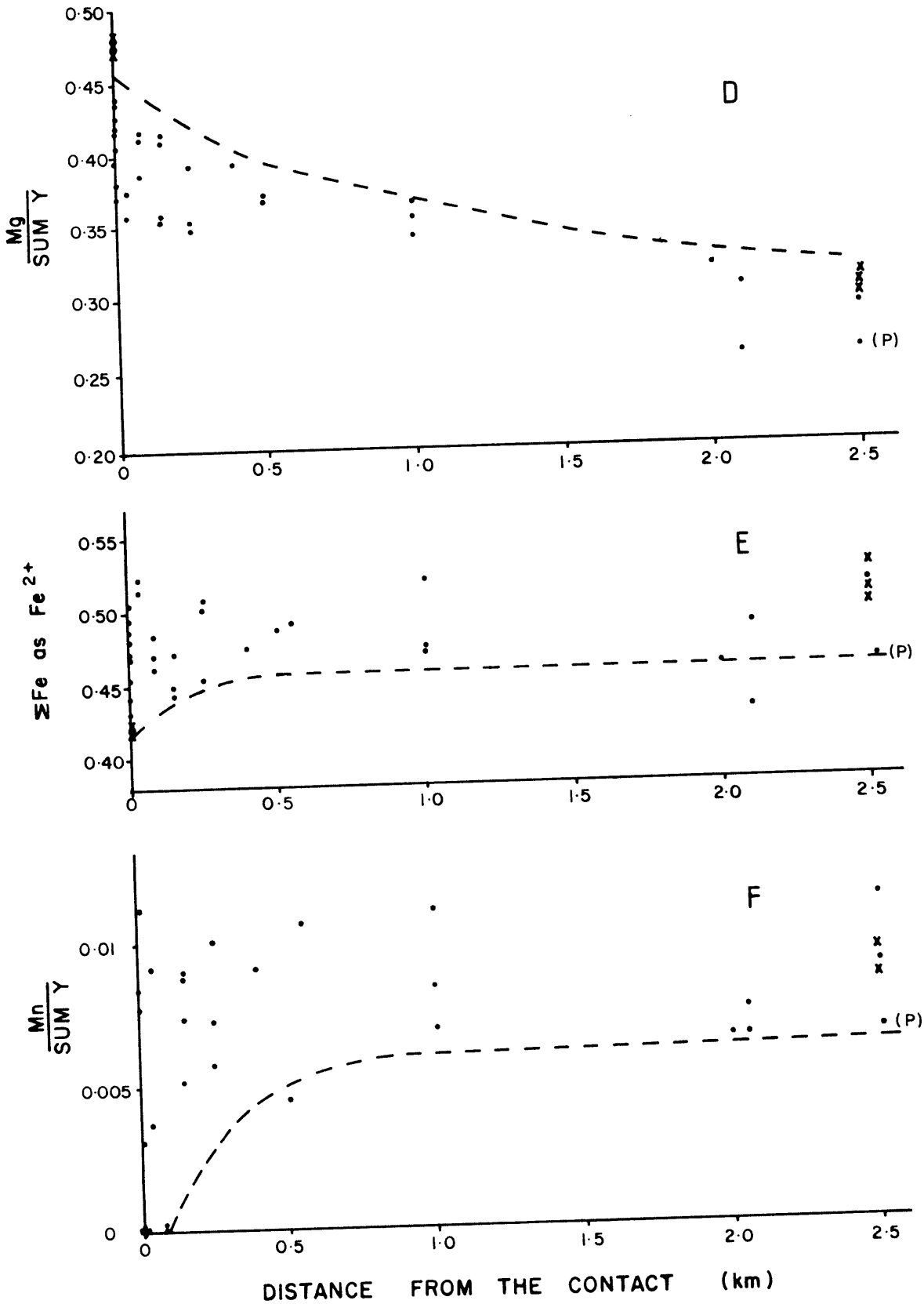
D
E
F
$\frac{Mg}{SUM\ Y}$
ΣFe as Fe^{2+}
$\frac{Mn}{SUM\ Y}$
(P)
0·50
0·45
0·40
0·35
0·30
0·25
0·20
0·55
0·01
0·005
0
0·5
1·0
1·5
2·0
2·5
DISTANCE FROM THE CONTACT (km)

lateral dimension of the tetrahedral layer). Charge balance in the octahedral layer must also be maintained. Consequently, certain trends can be correlated between the substituting elements. As expected from Fig. 3-4, graphs of both X_{Ti} (the atomic ratio of Ti to the sum of octahedral elements, Y) and X_{Mg} against $X_{Al^{VI}}$ (Figs. 3-5A and 3-5B respectively) show negative trends, though a greater spread of points occurs in the latter. Figs. 3-4C and D show a general increase in both Mg and Ti with increasing grade, and although this can be seen in the graph of X_{Mg} versus X_{Ti} (Fig. 3-5C), there also appears to be a negative trend between these elements at any particular distance from the contact. This latter trend is consistent with the results of Guidotti *et al.* (1977) and Gorbatschev (1968,1977) (i.e. a negative correlation between Mg and Ti at constant Al) for the more restricted variation in Al occurring at a given grade. A broad negative correlation also occurs between X_{Fe} and X_{Mg} (Fig. 3-5D).

With increasing grade throughout the aureole, the dominant substitution appears to increasingly favour the replacement of Al by Mg and Ti. The cause (or causes) of this grade-related change will be discussed in Section 3.6. This present discussion is concerned only with the manner in which this substitution has taken place with regard to the biotite chemistry. This can be studied by comparing specific biotite analyses at higher grades with Al-rich biotites at the outer limit of the aureoles (Table 3.4). The typical form of this substitution is

$$1\ Mg^{2+} + 1\ Ti^{4+} \rightleftarrows 2\ Al^{3+} \qquad (A)$$

as shown by most of the biotites in Table 3.4. Though this preserves charge balance, consideration of atomic radii (from Whittaker and Muntus (1970): Al - 0.61Å, Ti - 0.68Å; Mg - 0.80Å) suggest that such substitution enlarges the octahedral layer, and to compensate the Fe (radius 0.86Å) content of the biotite decreases slightly. Substitution of this type can give high-grade biotites with practically no Al^{VI} ($\lesssim$ 0.05 cations per formula unit) (e.g. Table 3.4, samples 291 and C42A). However, the decrease in Al content of the biotite is not always associated with an equal increase in the Mg and Ti (as in substitution A). This is believed to be related to variation in the host-rock chemistry affecting the relative availability of Mg and Ti at the site of biotite growth. If both Mg and Ti are readily available, substitution appears to take place as in A. However, to maintain

Figure 3-5: Correlations between the elements substituting in the biotite octahedral layer.

Symbols:
- ● Brown Biotite
- ●(P) Pale-brown Biotite
- × Green Biotite
- C42AX High-grade Green Biotite

Sum Y = Total number of ions in the octahedral layer.

The lines labelled in Figure 3-5C broadly delineate the negative correlation between Mg/Sum Y and Ti/Sum Y for the scatter of points at any particular distance from the contact.

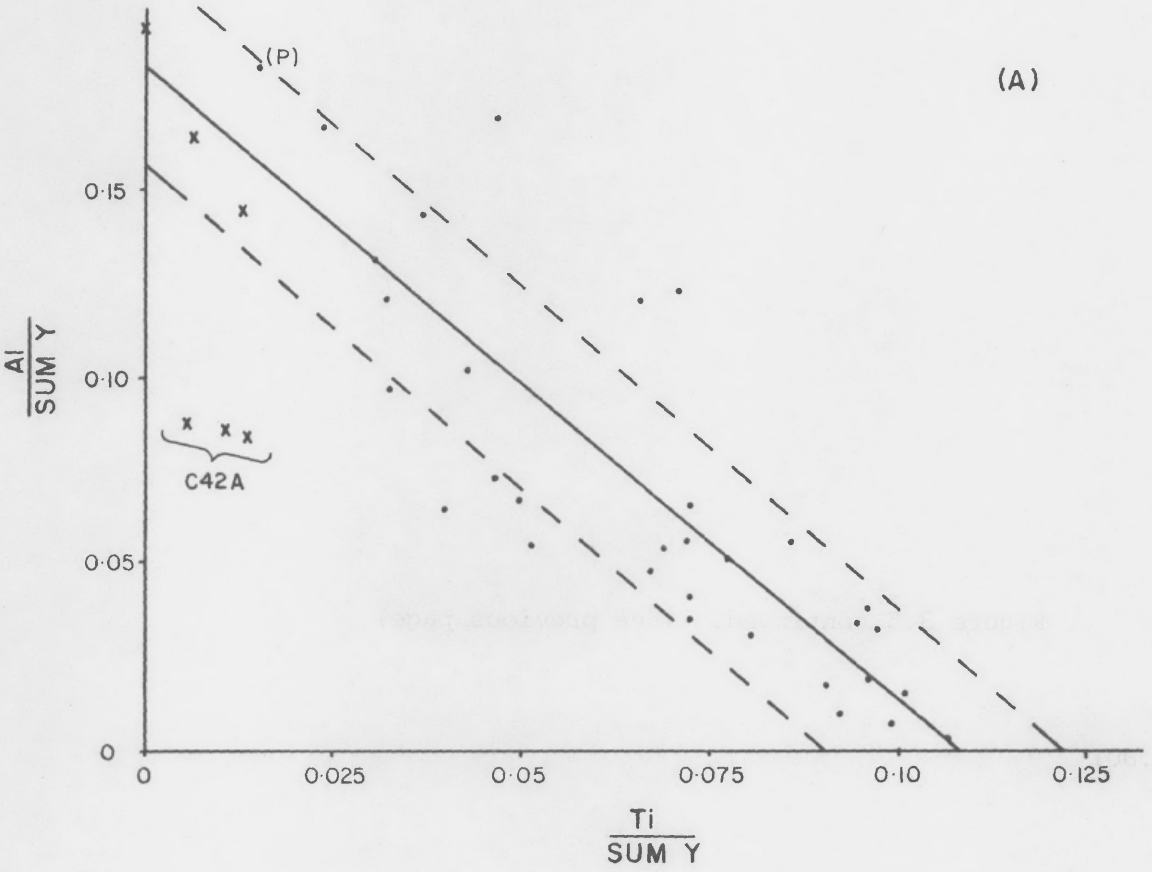
(A)
(P)
C42A
0·15
0·10
0·05
0
0·025
0·05
0·075
0·10
0·125
Al / SUM Y
Ti / SUM Y

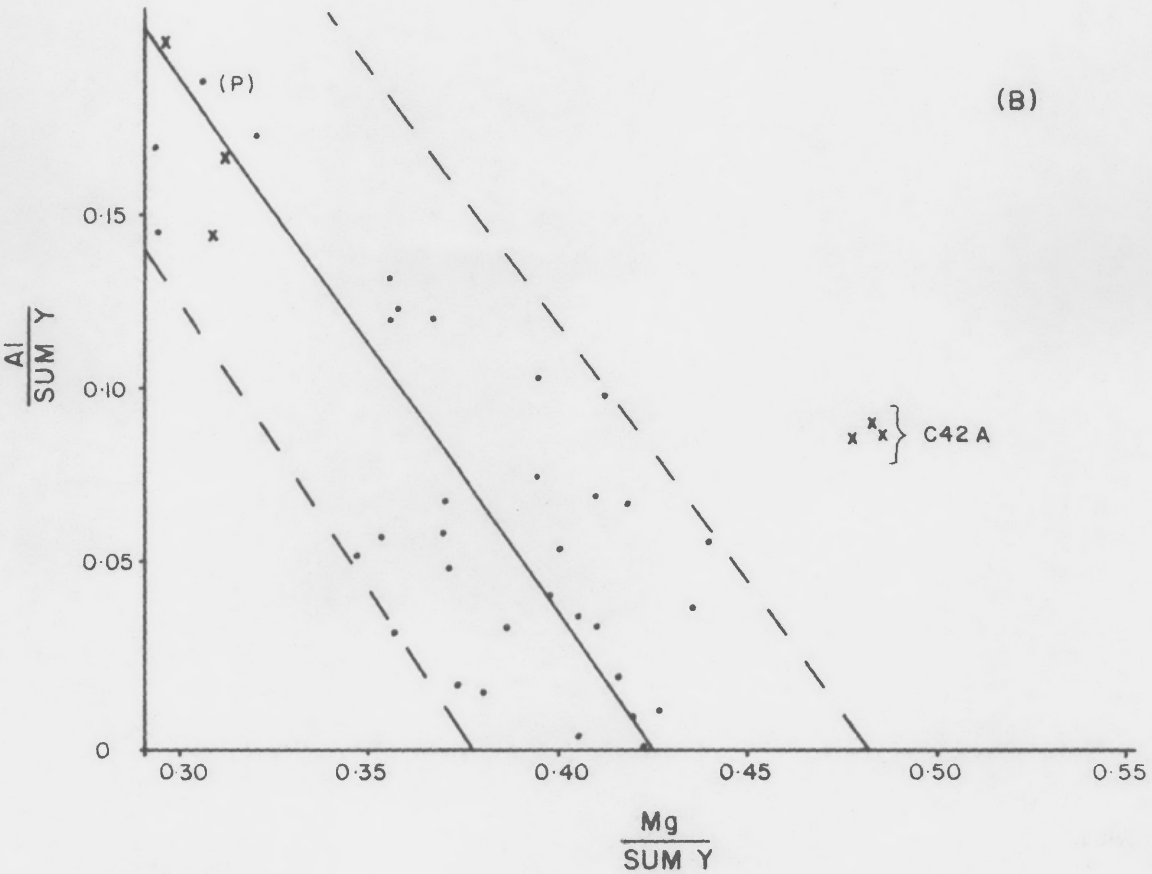
(B)
(P)
C42A
0·15
0·10
0·05
0
0·30
0·35
0·40
0·45
0·50
0·55
Al / SUM Y
Mg / SUM Y

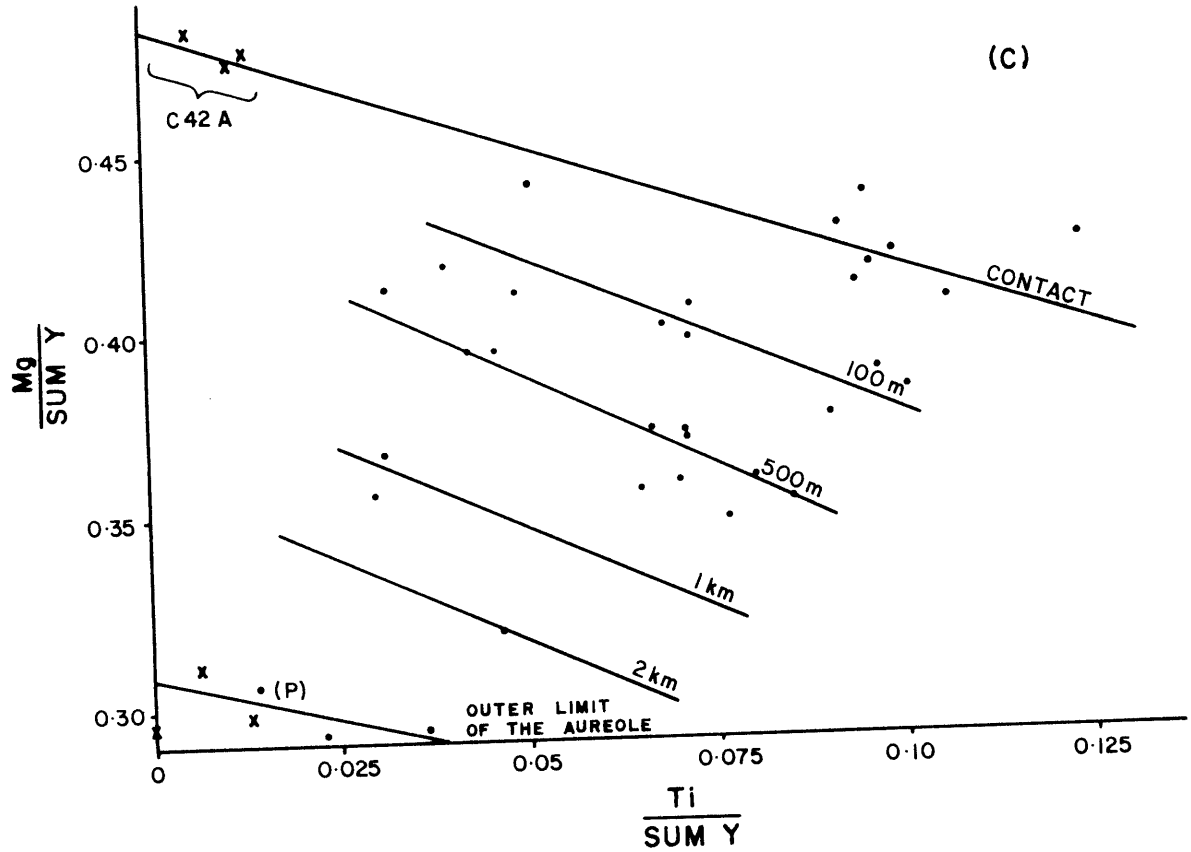
(C)
C42 A
CONTACT
100m
500m
1km
2km
(P)
OUTER LIMIT
OF THE AUREOLE
0·45
0·40
0·35
0·30
0
0·025
0·05
0·075
0·10
0·125
Mg / SUM Y
Ti / SUM Y

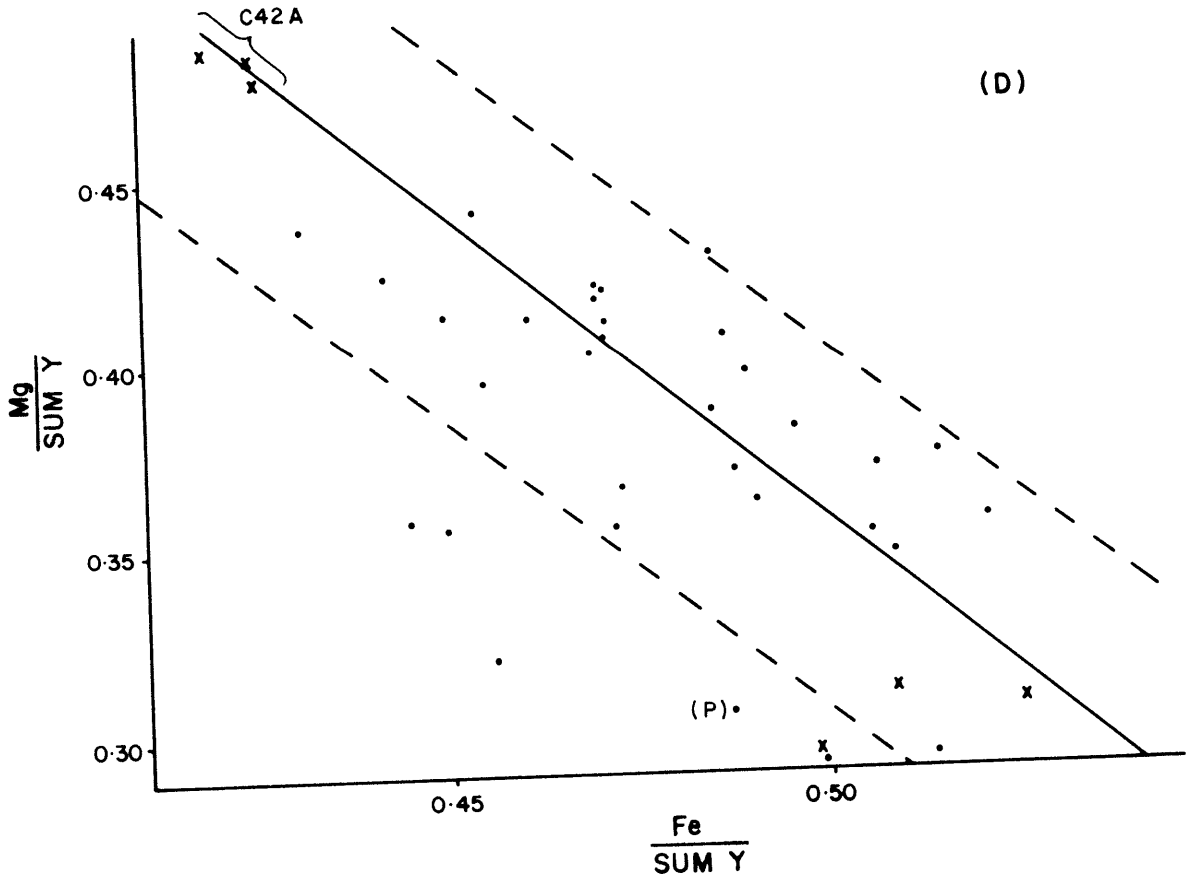
(D)
C42 A
(P)
0·45
0·40
0·35
0·30
0·45
0·50
Mg / SUM Y
Fe / SUM Y

TABLE 3.4. Variations in biotite chemistry with increasing grade in the Mt Duval Adamellite and Uralla Granodiorite aureoles

SAMPLE No.	30416					68		137A	63	164		291		C42A		187		C42A	
DISTANCE*	2.5km					1km		500m	500m	80m		CONTACT		CONTACT		CONTACT		CONTACT	
COMMENT†	Al-rich biotites from the outer limit of the aureole					A-TYPE SUBSTITUTION										B-TYPE	SUB-	C-TYPE	SUB-
SiO_2	35.79	35.13	35.86	36.30	36.15	36.01	38.44	36.43	36.17	35.74	35.45	35.21	35.51	35.93	35.90	36.77	36.56	35.72	34.81
TiO_2	-	0.33	0.65	1.15	1.86	1.51	1.58	3.55	3.47	4.63	4.77	6.13	4.79	5.22	4.53	5.04	3.37	0.57	0.30
Al_2O_3	20.15	19.75	17.91	18.79	18.85	17.73	15.78	14.93	14.89	14.62	14.81	13.34	13.62	13.83	13.89	14.24	14.74	16.79	17.01
FeO**	22.77	23.71	23.49	22.09	23.32	21.12	21.13	21.90	21.09	20.35	21.41	19.59	20.41	21.33	20.72	22.35	22.91	19.48	19.65
MnO	0.43	0.39	0.43	0.78	0.50	0.49	0.37	0.47	0.19	-	-	0.49	0.13	-	-	0.37	0.34	-	
MgO	7.57	8.14	7.71	7.25	7.47	8.91	9.19	9.21	8.96	10.15	9.56	10.53	10.24	10.02	10.55	9.63	9.39	12.61	12.52
CaO	0.12	0.17	0.14	0.13	-	-	-	-	-	-	-	-	-	-	-	0.08		-	
Na_2O	-	-	-	0.26	-	0.19	-	-	0.35	-	-	0.27	0.17	0.17	0.22	-		0.38	0.29
K_2O	7.99	7.62	9.30	9.04	9.40	9.17	8.77	9.14	9.25	9.27	9.20	9.61	9.64	9.77	9.93	9.49	8.99	9.51	9.54
Total	94.82	95.24	95.49	95.79	97.55	95.13	95.26	95.63	94.37	94.76	95.20	95.17	94.51	96.27	95.74	97.97	96.30	95.06	94.12
Structural formulae based on 22 oxygens																			
Si	5.501	5.404	5.558	5.559	5.466	5.539	5.855	5.610	5.632	5.523	5.481	5.451	5.538	5.515	5.532	5.548	5.608	5.476	5.408
Al^{IV}	2.499	2.596	2.442	2.441	2.534	2.461	2.145	2.390	2.368	2.477	2.519	2.436	2.462	2.485	2.468	2.452	2.392	2.524	2.592
Al^{VI}	1.155	0.988	0.832	0.953	0.829	0.755	0.690	0.321	0.367	0.188	0.182	-	0.044	0.018	0.056	0.083	0.274	0.512	0.525
Ti	-	0.038	0.076	0.133	0.212	0.175	0.181	0.411	0.406	0.538	0.555	0.714	0.562	0.603	0.525	0.572	0.389	0.066	0.035
Fe^{2+}	2.927	3.050	3.045	2.829	2.949	2.717	2.692	2.820	2.747	2.630	2.769	2.536	2.662	2.738	2.670	2.821	2.939	2.498	2.553
Mn	0.056	0.051	0.056	0.101	0.064	0.064	0.048	0.061	0.025	-	-	0.064	0.017	-	-	0.047	0.044	-	
Mg	1.734	1.866	1.781	1.655	1.683	2.042	2.086	2.114	2.079	2.338	2.203	2.429	2.380	2.292	2.423	2.166	2.147	2.881	2.899
Ca	0.020	0.028	0.023	0.021	-	-	-	-	-	-	-	-	-	-	-	0.013		-	
Na	-	-	-	0.077	-	0.057	-	-	0.106	-	-	0.081	0.051	0.051	0.066	-		0.113	0.087
K	1.567	1.496	1.839	1.766	1.814	1.799	1.704	1.796	1.838	1.828	1.815	1.898	1.918	1.913	1.952	1.827	1.759	1.860	1.891
Total cations	15.458	15.517	15.652	15.536	15.550	15.609	15.401	15.523	15.568	15.522	15.523	15.609	15.634	15.615	15.692	15.528	15.552	15.930	15.990
Y-GROUP	5.872	5.993	5.789	5.671	5.737	5.753	5.697	5.728	5.624	5.694	5.708	5.744	5.665	5.651	5.674	5.688	5.793	5.957	6.012
X-GROUP	1.587	1.524	1.862	1.865	1.814	1.856	1.704	1.796	1.943	1.828	1.815	1.979	1.970	1.964	2.018	1.840	1.759	1.973	1.978
Mg/Mg+Fe	0.372	0.380	0.369	0.369	0.363	0.429	0.563	0.428	0.431	0.471	0.443	0.489	0.472	0.456	0.476	0.434	0.422	0.536	0.532
Ti/SUM Y	-	0.006	0.013	0.023	0.037	0.030	0.032	0.072	0.072	0.095	0.097	0.124	0.099	0.107	0.092	0.101	0.067	0.011	0.006
Colour	G	G	G-B	Pale-B	B	B	B	R-B	R-B	R-B	R-B	R-B	R-B	R-B	R-B	R-B	R-B	G	G

* Distance from the igneous contact

† See text for substitution (sub) types

** All Fe as FeO

Colour abbreviations: G = green, G-B = green-brown, B = brown, R-B = red-brown

charge balance if Mg is limited relative to Ti, substitution is of the form

$$\tfrac{1}{2}\ Mg^{2+} + 1\tfrac{1}{2}\ Ti^{4+} \rightleftarrows 2\ Al^{3+} \qquad (B).$$

Although this type of substitution causes the average cation size to increase (as in A), the total number of octahedral ions is decreased, which leaves the lateral dimension of the octahedral layer broadly unaltered. Thus, this substitution requires relatively little adjustment in Fe content (e.g. Table 3.4, sample 187). Alternatively, if Ti is limited relative to Mg substitution occurs as

$$2\ Mg^{2+} + \tfrac{1}{2}\ Ti^{4+} \rightleftarrows 2\ Al^{3+} \text{ or } 3\ Mg^{2+} \rightleftarrows 2\ Al^{3+} \qquad (C).$$

Such substitution readily increases the layer size and consequently requires a significant decrease in Fe content (e.g. Table 3.4, sample C42A green biotite).

In summary, the change in biotite chemistry with increasing grade occurs with little change in both the charge and lateral dimension of the octahedral layer (thus requiring distinct correlations to exist between the substituting elements). The manner in which this takes place is dependent on small-scale variations in host-rock chemistry, and implies that these original small-scale chemical variations are maintained during metamorphism.

Biotite colour in relation to its chemistry and grade has been discussed by numerous authors. The most widely accepted controlling factors, as discussed by Hayama (1959) and Gorbatschev (1972), are Ti content and the oxidation ratio ($Fe_2O_3/FeO+Fe_2O_3$). The biotites of this study appear to support this conclusion, although the lack of Fe^{3+} data has prevented a complete investigation. The strong correlation between biotite colour and Ti content is seen in Fig. 3-4B and Table 3.4. In Fig. 3-4B green biotites are shown as crosses, and all green biotites have Ti/SUM Y values below 0.015, whereas the brown biotites plot above this value. In terms of weight percent TiO_2, green biotite typically contains less than 0.6%, green-brown about 0.65%, brown 1-2%, and the red-brown biotite greater than 2.5%. Oxidation ratios of the biotite separates are less than 0.1, for which the above correlation of colour with TiO_2 shows excellent agreement with the results of Hayama (1959) and Gorbatschev (1972).

3.5.4 Orthopyroxene

Characteristically, the orthopyroxene contains very little Al, Ti, or Fe^{3+} (a typical analysis of orthopyroxene is shown in Table 3.6). It commonly has a Mg/Mg+Fe ratio of about 0.45, though small variations are noted that appear to be related to changes in the coexisting biotite composition (discussed in Section 3.6).

3.5.5 Ilmenite

The titanium content of ilmenite remains relatively constant (approx. 2 cations per formula unit on the basis of 6 oxygens) with increasing grade. However, the Mn/Mn+Fe ratio of ilmenite shows a strong relationship with grade-related change in mineral assemblage (Table 3.5).

Outside the aureole, where it coexists with chlorite, the ilmenite is relatively Mn poor. The Mn content of ilmenite is much higher in the biotite zones, but it decreases markedly with the incoming of orthopyroxene. This is due to differences in the relevant distribution coefficients involving ilmenite (Table 3.5 and discussed further in Section 3.6).

3.5.6 Retrograde Chlorite

Retrograde chlorite, after biotite, occurs in the high-grade rocks. It is chemically distinguishable from chlorite outside the aureole by its slightly higher Mg/Mg+Fe ratio. This ratio in the retrograde chlorite reflects that of the high-grade biotite (Tables 3.4 and 3.6).

3.5.7 Retrograde Amphiboles

Retrograde amphibole is commonly associated with high-grade orthopyroxene. The amphibole is dominantly cummingtonite, displaying Mg/Mg+Fe ratios (about 0.45) and Mn contents very similar to those of the orthopyroxene it replaces (typical analyses are shown in Table 3.6). A pale-green actinolitic hornblende (after Leake, 1978) is often associated with the cummingtonite, and apart from its higher Ca content, it has higher Al and a higher Mg/Mg+Fe ratio (about 0.61) than either the cummingtonite or orthopyroxene. It also contains higher Ti, Fe^{3+} and Na than in the other two phases (Table 3.6). The actinolitic-hornblende cannot have formed from the orthopyroxene without a significant contribution of elements from accompanying phases. One such phase could be calcic feldspar, which

TABLE 3.5. Distribution coefficients for Mn between mineral pairs involving Ilmenite

SAMPLE	Mn/Mn+Fe		$K_{D(Mn)}$	
OUTSIDE THE AUREOLE	CHLORITE	ILMENITE		
C49	0.0152	0.0701	0.204	Chl-Il Av. $K_{D(Mn)}$
C49	0.0135	0.0839	0.150	= 0.176
30423	0.0185	0.0970	0.175	
BIOTITE ZONES	BIOTITE	ILMENITE		
140	0.0131	0.2869	0.033	
169	0.0159	0.1868	0.071	Bi-Il Av. $K_{D(Mn)}$
169	0.0159	0.1842	0.072	= 0.052
63	0.0091	0.2148	0.034	
OPX+BI ZONE	ORTHOPYROXENE	ILMENITE		
164	0.0237	0.0234	1.014	
187	0.0342	0.0441	0.767	O-Il Av. $K_{D(Mn)}$
291	0.0182	0.0408	0.435	= 0.877
C42A	0.0244	0.0190	1.291	

The distribution coefficient (K_D) for Mn between biotite (Bi) and ilmenite (Il), for example, is defined by:

$$K^{Bi\text{-}Il}_{D(Mn)} = \frac{X^{Bi}_{Mn}}{1-X^{Bi}_{Mn}} \times \frac{1-X^{Il}_{Mn}}{X^{Il}_{Mn}}$$

where X_{Mn} represents the atomic ratio Mn/Mn+Fe in the biotite and ilmenite.

TABLE 3.6. Microprobe analyses of retrograde amphiboles and chlorite

	RETROGRADE AMPHIBOLES		OPX†	RETROGRADE CHLORITE	
	C42A Cumm	C42A ACT-HB	C42A	165	291
SiO_2	50.79	50.19	49.93	26.67	26.95
TiO_2	0.12	0.35	-	-	0.14
Al_2O_3	0.98	4.71	0.62	18.55	19.61
Fe_2O_3*	1.30	5.25	0.97		
FeO	28.67	14.17	33.27	27.33	26.28
MnO	0.87	0.86	0.75	0.60	0.24
MgO	13.25	12.76	14.97	14.22	14.87
CaO	0.74	10.90	0.50	-	0.05
Na_2O	-	0.68	-	0.92	0.50
K_2O	-	0.28	-	-	0.06
Total	96.72	100.15	101.01	88.29	88.69
Structural formulae					
No. of oxygens	23	23	6	28	28
Si	7.777	7.248	1.953	5.676	5.645
Al^{IV}	0.177	0.752	0.029	2.324	2.355
Al^{VI}	-	0.050	-	2.328	2.486
Ti	0.014	0.038	-	-	.022
Fe^{3+}	0.149	0.571	0.029		
Fe^{2+}	3.672	1.711	1.089	4.863	4.602
Mn	0.113	0.105	0.025	0.107	0.043
Mg	3.024	2.746	0.873	4.512	4.642
Ca	0.121	1.687	0.021	-	0.011
Na	-	0.190	-	0.378	0.201
K	-	0.052	-	-	0.015
Total cations	15.047	15.150	4.018	20.187	20.022

* Fe_2O_3 calculated by the method of Papike *et al.* (1974).

† Prograde orthopyroxene shown for comparison with the amphiboles.

Prograde biotite - see Table 3.4.

Abbreviations CUMM = cummingtonite, ACT-HB = actinolitic hornblende, OPX = orthopyroxene.

would contribute the required Ca and Al.

3.6 METAMORPHIC REACTIONS AND PHASE RELATIONS

Contact-metamorphic reactions and phase relations are described in detail after a brief discussion of the reactions related to regional metamorphism.

3.6.1 Reactions of Regional Metamorphism

Greywackes outside the contact aureole have been reconstituted by very low-grade regional metamorphism. The major product of this metamorphism is the fine-grained aggregates of chlorite + sphene present amongst the detrital crystal and lithic fragments. Much of the chlorite and sphene exists as thin films along the grain boundaries, and possibly represents the remains of a more abundant clay-size matrix present before compaction and regional metamorphism. The abundance of chlorite in the matrix material of volcanically derived greywackes has been noted by Williams *et al.* (1954, p.303). The chlorite may also have been derived from the alteration of more-basic volcanic rock fragments, or original volcanic glass. Evidence for the origin of this chlorite is speculative due to its fine grainsize. However, in the greywackes outside the aureole, aggregates of coarse-grained chlorite and sphene occur within partial remains of detrital amphibole, suggesting that much of the coarser-grained chlorite and sphene has formed from precursor amphibole. As ilmenite and plagioclase are common phases in these rocks the following equation, based on probe data, is suggested:

$$1.04 \text{ Actinolite} + 3.0 \text{ Anorthite} + 4.06 \text{ Ilmenite} + 7\ H_2O \rightarrow 1.0 \text{ Chlorite} + 2.54 \text{ Sphene} + 3.64 \text{ Quartz} \qquad (3\text{-I})$$

REACTANTS

Actinolite $Ca_2Fe_{1.30}Mg_{3.70}Mn_{.04}Si_8O_{22}(OH)_2$

Ilmenite $Fe_{.99}Mn_{.01}TiO_3$

PRODUCTS

Chlorite $Al_{2.7}Fe_{5.20}Mg_{3.85}Mn_{.08}Si_{5.6}Al_{2.4}O_{20}(OH)_{16}$

Sphene $Ca_2Ti_{1.60}Al_{.35}Fe_{.05}Si_2O_{10}$

This reaction could represent the breakdown of amphibole occurring both as discrete grains, and in lithic fragments. Much of the amphibole

itself may be the alteration product of original pyroxene.

Regional metamorphism is also believed to be responsible for the alteration of detrital biotite (possibly to Fe-vermiculite, Section 3.3), and for the sericitisation of plagioclase. From probe analyses of the phases involved, the elements released by the biotite alteration, namely K, Al and Si, are those required for sericitisation of plagioclase. Therefore, these changes may occur as a coupled reaction, represented by equation 3-II:

1.0 Biotite + 4.62 Anorthite + 0.46 Hematite + 0.58 Quartz + 2.06 H_2O
→ Sericite + 2.0 Epidote + 0.5 Vermiculite + 0.39 Sphene (3-II)

REACTANTS

Biotite $K_{1.8}Fe_{2.6}Mg_{1.75}Mn_{.03}Ti_{.6}Al_{.5}Si_{5.6}Al_{2.4}O_{20}(OH)_4$

PRODUCTS

Sericite $K_{1.75}Al_{3.88}Si_{6.2}Al_{1.8}O_{20}(OH)_4$

Epidote $Ca_{1.92}Fe^{3+}_{.75}Al_{2.25}Si_3O_{12}(OH)$

Vermiculite $Fe^{3+}_4Mg_{3.4}Mn_{.06}Si_{4.5}Al_{3.5}O_{20}(OH)_4$

Sphene $Ca_2Ti_{1.55}Al_{.35}Fe_{.05}Si_2O_{10}$

3.6.2 Reactions and Phase Relations of Contact Metamorphism

Biotite Isograd.

From the mineralogical changes associated with the incoming of biotite (Section 3.4.1), it appears that chlorite, sphene and K-feldspar are the major reactants in the formation of biotite. From probe data on these and associated phases, the following equation is suggested:

1.0 Chlorite + 4.6 K-feldspar + 0.42 Sphene + 3.5 Plagioclase(1) + 0.75 Hematite
= 2.26 Biotite + 4.8 Plagioclase(2) + 0.2 Ilmenite + 5 Quartz + 3.5 H_2O (3-III)

REACTANTS

Chlorite $Al_{2.7}Fe_{5.2}Mn_{.08}Mg_{3.85}Si_{5.5}Al_{2.5}O_{20}(OH)_{16}$

K-feldspar $K_{.9}Na_{.1}AlSi_3O_8$

Sphene $Ca_2Ti_{1.60}Al_{.35}Fe_{.05}Si_2O_{10}$

Plagioclase(1) $Na_{.9}Ca_{.1}Al_{1.1}Si_{2.9}O_8$

PRODUCTS

Biotite $K_{1.83}Al_{.84}Ti_{.2}Fe_{2.9}Mn_{.03}Mg_{1.7}Si_{5.4}Al_{2.6}O_{20}(OH)_4$

Plagioclase(2) $Na_{.75}Ca_{.25}Al_{1.25}Si_{2.75}O_8$

Ilmenite $Fe_{.91}Mn_{.09}TiO_3$

Observed modal changes (Table 3.3) are broadly consistent with the relative proportions of reactants and products proposed in equation 3-III. This reaction is further supported by the textural occurrence of biotite, which is identical to that of chlorite plus sphene outside the aureole. Rare examples can also be found at the biotite isograd of biotite occurring within patches of chlorite. Besides the decrease in modal abundance of K-feldspar crystal fragments (Table 3.3), the decrease in K-feldspar at this boundary is evidenced by the disappearance of rhyolite fragments possessing a spherulitic texture (Section 3.4.1). Direct evidence of the change in plagioclase composition is not available, but is inferred from the decrease in modal amount of albite (Ab > 90) and anorthoclase (Ab > 63). The proposed alteration of albite, and the albite component of anorthoclase, to a more-calcic plagioclase is believed to be related to the liberation of Ca from the breakdown of sphene, and the release of Al from the formation of biotite after chlorite. (The breakdown of anorthoclase also releases K used in the formation of biotite). The general decrease in alkali feldspars (including albite) and formation of more-calcic feldspar associated with the incoming of biotite is also likely to have occurred within the volcanic fragments.

The abrupt incoming of biotite and immediate loss of chlorite + K-feldspar is indicative of a discontinuous reaction (as outlined in Section 2.7). Therefore, iron oxide is a necessary participant in the above reaction, because the biotite produced has a lower Mg/Mg+Fe ratio than the chlorite. Hence, biotite forms with a Mg/Mg+Fe ratio between those of the reactants chlorite and iron oxide (Fig. 3-6), and continues to form at constant temperature until one of the reactants (typically chlorite) is exhausted. This type of reaction involves no continuous compositional adjustment of the ferromagnesians over a temperature interval. Similarly, the biotite has Al/Al+Ti ratios between those of sphene and chlorite (Fig. 3-7). The lowest-grade biotite has high Al/Al+Ti values, reflecting the composition of the chlorite. However, this ratio decreases with increasing temperature, as described in Section 3.5.

Figure 3-6: Schematic T-X(Fe-Mg) diagram for the greywackes in the Mt Duval Adamellite and Uralla Granodiorite contact aureoles.

Points represent specific microprobe analyses.

Symbols: ● Biotite

× Orthopyroxene

■ Chlorite

$K_{D(Mg)}^{Bi-O}$ (defined in the text and Table 3.5) values for three mineral pairs are shown in the diagram.

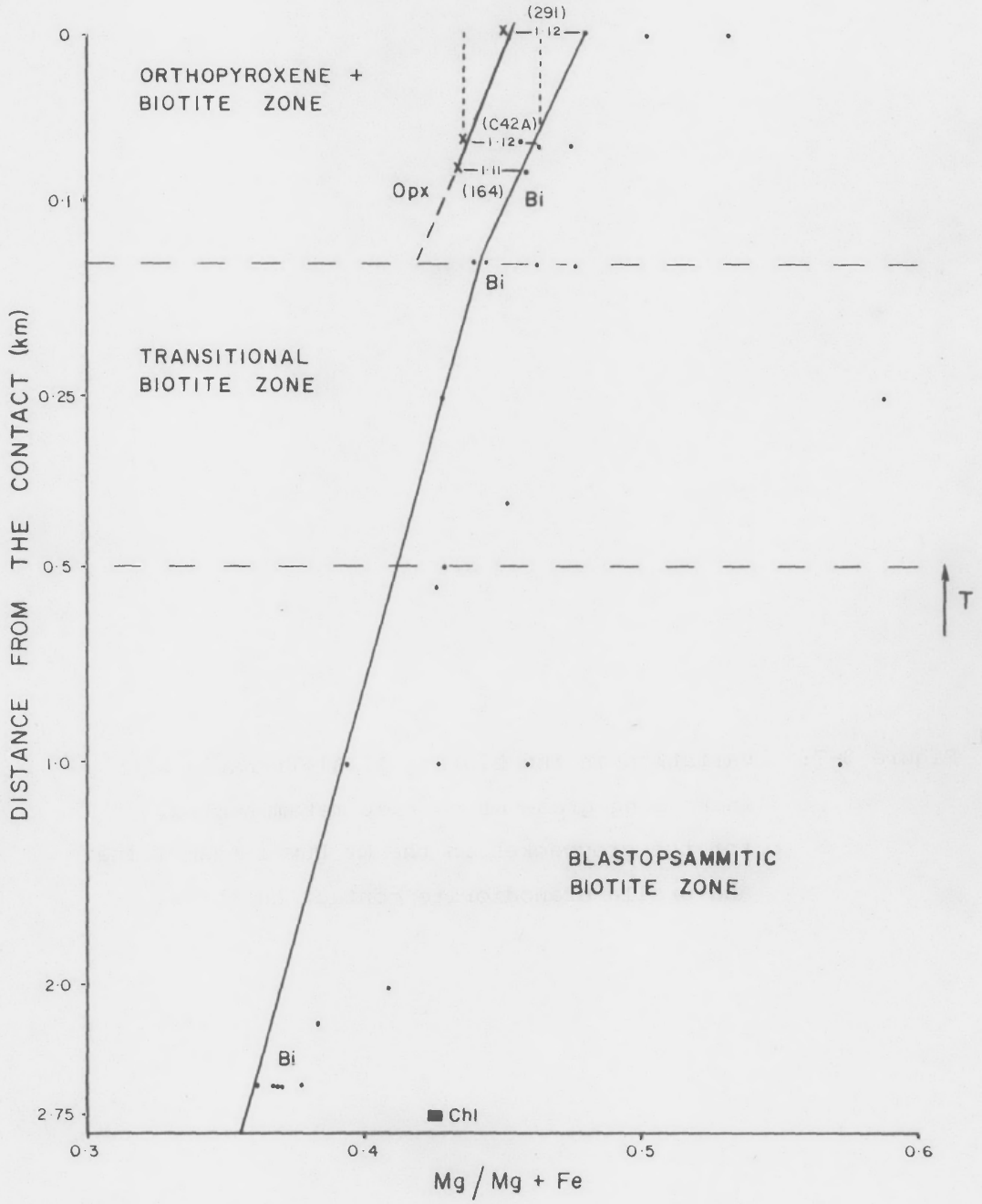
(291)
1·12
ORTHOPYROXENE +
BIOTITE ZONE
(C42A)
1·12
1·11
Opx
(164)
Bi
Bi
TRANSITIONAL
BIOTITE ZONE
T
BLASTOPSAMMITIC
BIOTITE ZONE
Bi
Chl
DISTANCE FROM THE CONTACT (km)
0
0·1
0·25
0·5
1·0
2·0
2·75
0·3
0·4
0·5
0·6
Mg / Mg + Fe

Figure 3-7: Variation in the biotite Al/Al+Ti ratio with increasing grade of contact metamorphism, for the greywackes in the Mt Duval Adamellite and Uralla Granodiorite contact aureoles.

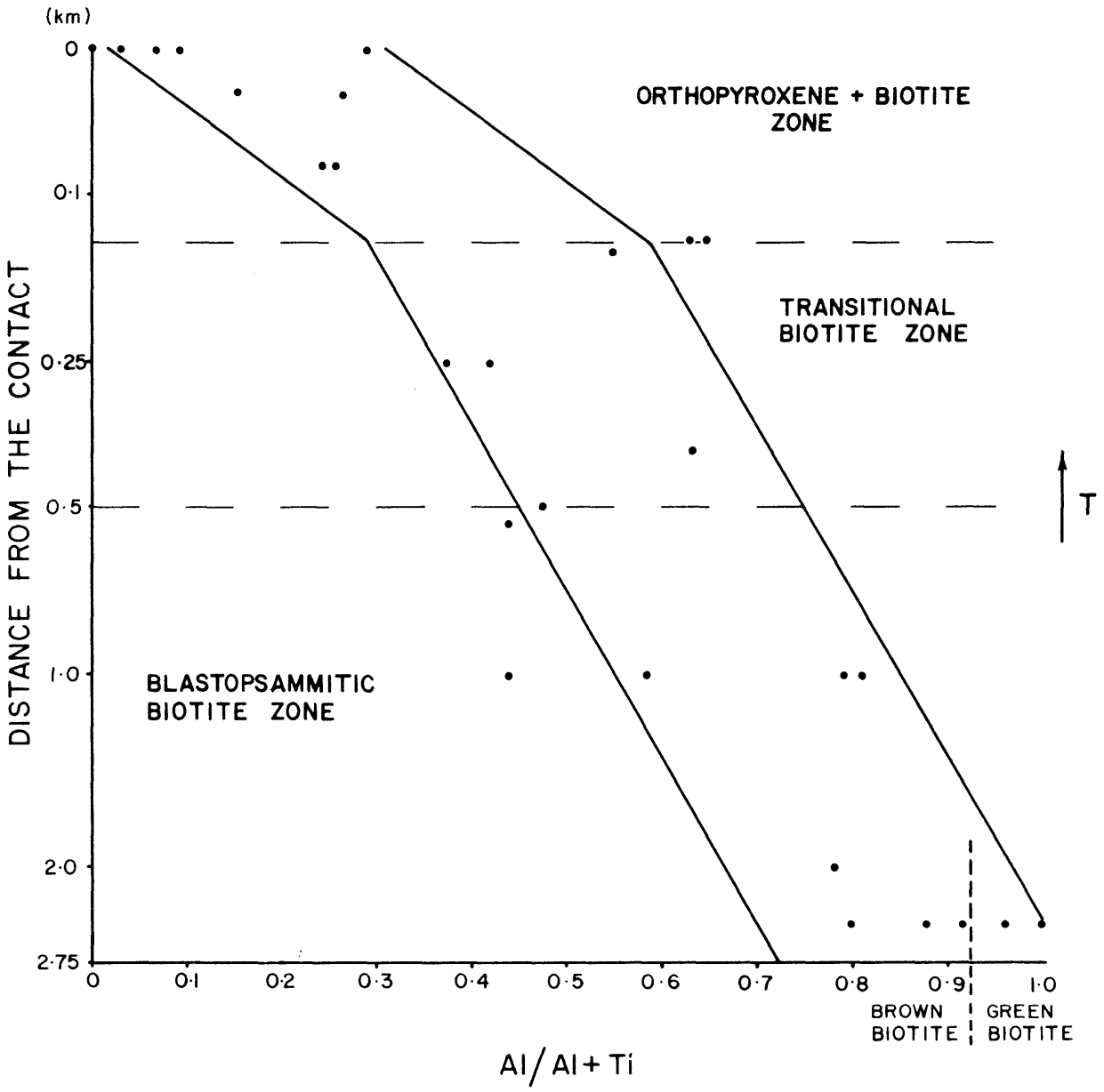
(km)
0
0·1
0·25
0·5
1·0
2·0
2·75
DISTANCE FROM THE CONTACT
ORTHOPYROXENE + BIOTITE ZONE
TRANSITIONAL BIOTITE ZONE
BLASTOPSAMMITIC BIOTITE ZONE
T
0
0·1
0·2
0·3
0·4
0·5
0·6
0·7
0·8
0·9
1·0
BROWN BIOTITE
GREEN BIOTITE
Al/Al+Ti

To represent the iron oxide in equation 3-III as entirely hematite is a simplification to facilitate balancing of the equation. This is because ilmenite becomes poorer in Fe^{2+} across the biotite isograd (Section 3.5), and iron liberated from the ilmenite would probably be involved in the formation of biotite. The change in ilmenite composition is related to the lower $K_{D(Mn)}$ value (defined in Table 3.5) for coexisting biotite and ilmenite compared with that for chlorite and ilmenite (Table 3.5). Minor phases such as epidote and vermiculite are also lost at the biotite isograd. Therefore, other less prominent reactions must be occurring with reaction 3-III, to fully accomplish the observed mineralogical changes.

Transitional Biotite Zone.

The transitional biotite zone is delineated by textural rather than mineralogical changes, and no isograd is defined at the low-grade boundary of this zone. However, there has been a gradual change in biotite composition across the blastopsammitic biotite zone (Section 3.5.3), and biotite within the transitional biotite zone is poorer in Al and richer in both Ti and Mg than that formed at the biotite isograd. The changes in biotite chemistry (Mg/Mg+Fe and Al/Al+Ti) with respect to these zones are shown in Figs. 3-6 and 3-7.

The change in biotite chemistry with increasing grade is accompanied by an increase in the Ca content (and hence Al content) of the feldspars. This is evidenced by the oligoclase-andesine composition of all newly formed plagioclase, in contrast to the albite and anorthoclase compositions of a significant proportion of relict feldspar grains and feldspar within the volcanic lithic fragments (Section 3.5.2). These changes are also associated with the breakdown of sphene (consistent with its modal decrease toward the contact; Section 3.4). Sphene breakdown liberates Ti, which increases in the biotite, and Ca (plus SiO_2), which appears to combine with Al, released from the biotite, to form the more-calcic feldspars. This redistribution of elements between the three phases (biotite-feldspar-sphene) also involves an increase in the modal amount of plagioclase and a minor decrease in biotite (as well as variations in the modal contents of K-feldspar and opaques), to maintain a complex balance of elements within these phases. These mineralogical trends continue until the ortho-pyroxene isograd is reached.

Orthopyroxene Isograd.

From the mineralogical changes occurring at this boundary (Section 3.4), and probe data for the appropriate phases, the orthopyroxene-forming reaction can be represented by equation 3-IV

2 Biotite(1) + 4.9 Quartz + 2 Plagioclase(1) + 0.27 Sphene + 0.15 Ilmenite(1) → Biotite(2) + 2 Orthopyroxene + 2 K-feldspar + 2.54 Plagioclase(2) + 0.75 Ilmenite(2) + 2 H_2O (3-IV)

REACTANTS

Biotite(1)	$K_{1.85}Na_{.1}Al_{.3}Ti_{.44}Fe_{2.7}Mn_{.02}Mg_{2.07}Si_{5.6}Al_{2.4}O_{20}(OH)_4$
Plagioclase(1)	$Na_{.9}Ca_{.1}Al_{1.1}Si_{2.9}O_8$
Sphene	$Ca_2Ti_{1.6}Al_{.35}Fe_{.05}Si_2O_{10}$
Ilmenite(1)	$Fe_{.8}Mn_{.2}TiO_3$

PRODUCTS

Biotite(2)	$K_{1.9}Ti_{.7}Fe_{2.6}Mg_{2.4}Si_{5.6}Al_{2.4}O_{20}(OH)_4$
Orthopyroxene	$Fe_{1.1}Mg_{.87}Mn_{.02}Si_2O_6$
K-feldspar	$K_{.9}Na_{.1}AlSi_3O_8$
Plagioclase(2)	$Na_{.7}Ca_{.3}Al_{1.3}Si_{2.7}O_8$
Ilmenite(2)	$Fe_{.96}Mn_{.04}TiO_3$

The molar proportions used in equation 3-IV are consistent with the observed modal changes in Table 3.3, which suggest a decrease in biotite of about half the increase in K-feldspar and orthopyroxene (allowing for different molar volumes of the phases). The coexistence of biotite and orthopyroxene in apparent equilibrium throughout the high-grade zone suggests that reaction 3-IV is continuous, and this is represented above by the presence of biotite on both sides of the equation.

$K_{D(Mg)}^{Bi-O}$ values (defined in Table 3.5), for coexisting biotite (Bi) and orthopyroxene (O) in these rocks, of 1.11 and 1.12 show the preference of Fe for orthopyroxene relative to biotite. Therefore, formation of the orthopyroxene requires an increase in Mg/Mg+Fe in the coexisting biotite. With increasing temperature, orthopyroxene continually forms at the expense of biotite, involving a progressive increase in Mg/Mg+Fe in both minerals. It is this continuous compositional adjustment of both reactants and

products, as the reaction proceeds over a temperature interval, which designates its continuous nature. This change is represented for three coexisting pairs in Fig. 3-6. $K_{D(Mg)}^{Bi-O}$ values for these pairs are also shown.

The incoming of orthopyroxene does not define a sharp boundary, because it is dependent not only on temperature, but also on the Mg/Mg+Fe ratio of the biotite. Consequently, the amount of orthopyroxene formed at a given temperature is also dependent on the composition of the lower-grade biotite.

The increase in Mg/Mg+Fe in the biotite with the incoming of orthopyroxene (primarily an increase in Mg; Figs. 3-4D and E) should be associated with a decrease in the biotite's Al+Ti content (Gorbatschev, 1968,1977, discussed in Section 3.5). With increasing grade across the orthopyroxene + biotite zone, a continuous decrease in the abundance of biotite is associated with an increase in its Ti content. In keeping with the biotite's required decrease in Al+Ti content, the increase in both the Mg/Mg+Fe ratio and Ti in the biotite is accompanied by a significant decrease in Al, with the Al being used in the formation of the coexisting plagioclase and K-feldspar (i.e. in the form of substitution A, Section 3.5). This results in a major decrease in the Al/Al+Ti ratio of biotite at the orthopyroxene + biotite zone boundary (Fig. 3-7). It is noted that the change in biotite chemistry associated with the continuous orthopyroxene-forming reaction is identical to that occurring in the cation exchange reaction between biotite, feldspar, and sphene at lower grade (merely causing the trends of decreasing Al and increasing Ti and Mg to be exaggerated in the high-grade zone, Fig. 3-4). In both types of reaction, Al decreases in the biotite and is incorporated into the coexisting feldspar.

Biotite within the high-grade zone also shows a decrease in Mn content (Fig. 3-4G), and is commonly Mn-free near the contact. This reflects the preference of Mn for the orthopyroxene structure relative to biotite. Ilmenite in this zone is also depleted in Mn relative to that in the biotite zones. This is because the $K_{D(Mn)}$ value for orthopyroxene and ilmenite is much higher than for biotite and ilmenite (Table 3.5).

An exception to the above discussion is the formation of green

(Ti-poor) biotite in sample C42A (Table 3.4) collected at the contact of the Uralla Granodiorite. Apparently it formed within inherently very Ti-poor domains of the rock. In these biotites, Mg has increased significantly (compared to lower-grade biotites, Fig. 3-4D). However, without the associated increase in Ti content, their Al contents have not decreased as markedly as in the red-brown biotite from the same rock (Table 3.4) (i.e. the biotite chemistry has changed according to substitution C, Section 3.5).

3.7 DISCUSSION OF BIOTITE CHEMISTRY AND ROCK TYPE

Prograde changes in biotite chemistry have been widely discussed in the literature. Various trends have been recognised that can be related to changes in the mineral assemblage, due to metamorphic reactions, or to changes in the distribution coefficients for coexisting phases. Therefore, the variations in biotite chemistry recognised within a given study are strongly dependent on the paragenesis of the rock type considered. The changes in biotite chemistry with increasing grade, characteristic of the psammitic rocks of the Mt Duval aureole, will now be briefly discussed in comparison with changes observed in the pelitic rocks of the Walcha Road aureole (Chapter Two), and changes in biotite chemistry noted by other authors.

The decreasing Al^{VI} content of biotite with increasing grade, associated with the greywackes studied here (Fig. 3-4C), does not occur in the pelites of the Walcha Road aureole, and has not been commonly reported by other authors. Binns (1969) noted a possible decrease in Al^{VI} with increasing grade, and related it to a complex relationship between biotite and coexisting muscovite or K-feldspar. Engel and Engel (1960) also suggested the Al^{VI} content of biotite may decrease with increasing grade in greywackes containing only localised minor muscovite. The general scarcity of recorded instances of this feature, though, is related to the use by most authors of pelitic assemblages to study variations in biotite chemistry.

Compared with typical pelites (e.g. Vallance, 1960; Atherton, 1968; sample 26213 in Table 2.1) greywackes of this study have lower Al and K, but higher Si, Ca and Na. Consequently, although the pelites are rich in muscovite outside the aureole and in the lower-grade zones, these

greywackes contain only rare muscovite and are rich in plagioclase. Similarly, higher-grade pelitic assemblages readily form Al-rich silicates, such as staurolite, cordierite, almandine and Al-silicates, whereas the greywackes remain rich in biotite and feldspar, and in the highest-grade zone contain orthopyroxene. In pelitic rocks, biotite is typically Al-rich (saturated in Al) and remains so with increasing grade. This was found within the Walcha Road aureole (Fig. 2-4B), and has also been described by a number of previous authors (e.g. Butler, 1967; Guidotti *et al.*, 1977; Yardley *et al.*, 1980). The Al content of biotite remains constant with variations in grade because it is buffered by the associated Al-rich silicates. The formation of other Al-containing phases with increasing grade apparently derives Al from the breakdown of the Al-rich silicates (e.g. muscovite), rather than by reducing the Al content of the biotite. However, in the greywackes, the limited amount of Al present is distributed between the coexisting feldspar and biotite. With increasing grade the formation of further Al-bearing phases (commonly further feldspar) reduces the Al content of the biotite.

As noted in Section 3.5.3, a negative relationship exists between the Al+Ti content of biotite and its Mg/Mg+Fe ratio (Gorbatschev, 1968, 1977). Therefore, changes in biotite Ti content, that occur with a shift in the Mg/Mg+Fe ratio of biotite in continuous reactions, are affected by changes in the biotite Al content. As changes in Al content are dependent on rock type (as described above), the variation in Ti content associated with continuous reactions must also depend on the rock type involved. With the incoming of garnet in the pelites of the Walcha Road aureole, the Mg/Mg+Fe ratio of the coexisting biotite is increased. As the biotite Al content remains constant in the pelites, the Ti content of the biotite is decreased. Conversely, with the incoming of orthopyroxene in the greywackes, although the Mg/Mg+Fe ratio of the biotite is again increased, so is its Ti content. This is because the biotite Al content is decreased markedly in the orthopyroxene-forming reaction, associated with the Al entering the coexisting feldspar.

3.8 P-T CONDITIONS

The mineralogy of the greywackes does not allow precise determinations of temperature and pressure. Shear pressure does not appear to

have been significant in the metamorphism of these sediments, as the minerals lack preferred orientation.

Load pressure is restricted to below 4-5 kb, as indicated by the presence, in associated rocks, of andalusite, wollastonite, and cordierite (Mg/Mg+Fe = 0.5) without garnet. However, pressures of 1 kb or less, associated with very shallow depths of emplacement, may be inferred if the intrusion of the Mt Duval Adamellite into a series of acid volcanics (the Annalee Pyroclastics) of similar age is taken as evidence of the pluton intruding its own volcanic pile.

As noted in Section 2.9, very little experimental work has been carried out on the temperature of biotite formation. Values of 300-400^{o}C are generally given for the incoming of biotite (Winkler, 1976; Turner, 1980), and such temperatures are believed to represent the outer limit of the Mt Duval aureole.

The higher-grade reaction 3-IV broadly represents the breakdown of biotite plus quartz to form orthopyroxene plus K-feldspar. Again, experimental results are limited and conflicting. Loomis (1966), with no supporting data or reference, stated that the reaction occurs at 720^{o}C at 1.4 kb. More recent information on the reaction is provided by Hoffer and Grant (1980) who, using biotite with intermediate Mg/Mg+Fe values, found that orthopyroxene formed from biotite plus quartz at 640^{o}C at 1.5 kb and that biotite coexisted with orthopyroxene up to 670^{o}C. Similarly, at 0.5 kb, the values were 560^{o}C and 610^{o}C respectively. Hoschek (1976) also ran experiments on the biotite plus quartz breakdown, studying it in association with varying plagioclase compositions. He found values ranging between 650^{o}C and 725^{o}C at 4 kb, which, if extrapolated to pressures around 1 kb, agree more closely with the results of Hoffer and Grant (1980) than those of Loomis (1966). Therefore, although speculative, it is believed that the incoming of orthopyroxene, for intermediate Mg/Mg+Fe values of biotite (as in this study), may well occur around 600^{o}C, for an estimated pressure of 1 kb in the Mt Duval aureole. Biotite and orthopyroxene coexist throughout the innermost zone, and therefore, from the above data, contact temperatures would not be expected to greatly exceed 650^{o}C. Consequently, an increase from between 300-400^{o}C up to approximately 650^{o}C appears to have occurred across the 2½km-wide aureole.

3.9 SUMMARY

A contact aureole 2½km wide has been identified around the Mt Duval Adamellite within an isochemical sequence of greywackes. Within this aureole a series of metamorphic changes can be related to a systematic increase in temperature toward the contact. Three distinct zones (distinguished by both texture and mineral assemblage) have been mapped parallel to the pluton perimeter. These are

I) Blastopsammitic Biotite Zone (2½ km - 500 m);

II) Transitional Biotite Zone (500 m - 150 m);

III) Biotite+Orthopyroxene Zone (150 m - contact).

The mineralogy outside the aureole has been modified, by very low-grade regional metamorphism, to give an assemblage containg chlorite + sphene. The outer limit of the aureole is taken as the incoming of biotite, formed by a discontinuous reaction involving breakdown of chlorite plus sphene. The outer zone shows very little textural adjustment of the original sediment, and the recognition of obvious textural modification defines the beginning of the second zone. The initial textural changes are coarsening of fine-grained lithic fragments and minor recrystallisation of coarser crystals. Such processes continue with increasing grade until original fragments are difficult to recognise. The high-grade zone is marked by the incoming of orthopyroxene and K-feldspar, associated with a decrease in biotite. This involves a continuous reaction which proceeds with adjustment of the Mg/Mg+Fe ratio of both the orthopyroxene and biotite. The incoming of orthopyroxene does not define a sharp isograd as it is dependent on both temperature and biotite composition. Texturally, the high-grade zone is totally reconstituted, leaving little trace of the original sedimentary appearance, and exaggerated grain growth results in the development of coarse xenoblastic grains.

Distinct variations occur in the biotite chemistry with increasing grade, related to changes in the mineral assemblage, and to changes in the distribution coefficients of coexisting phases. Compositional changes within the biotite are constrained by its structural (equal lateral dimensions for the octahedral and tetrahedral layers) and charge balance requirements. Therefore, correlations exist between variations in the elements substituting in the biotite. At the outer limit of the aureole,

biotite is Al-rich and Ti-poor, reflecting the chemistry of its precursor chlorite. Throughout the two outer zones the biotite gradually decreases in Al and increases in both Mg and Ti. This is related to a continuous cation exchange between biotite, plagioclase and sphene. The change in biotite chemistry is associated with an increase in both the modal amount and An content of the plagioclase, and a continuously decreasing modal amount of sphene. With the incoming of orthopyroxene and K-feldspar, the Mg/Mg+Fe ratio of the biotite is increased (primarily an increase in Mg). This is combined with a significant decrease in the Al content of biotite, and an associated increase in its Ti content. Hence, the changes in biotite chemistry at lower grade are further emphasised in the orthopyroxene + biotite zone. Mn content of the biotite also decreases in the high-grade zone, due to the preference for Mn to enter the orthopyroxene structure rather than that of biotite.

Biotite composition, however, is also dependent on its host-rock composition, which results in a significant variation in biotite chemistry at any given distance from the contact (i.e. grade). This variation can occur over a distance of a few mm, and implies that small-scale chemical variations within the greywackes are maintained during metamorphism. Three types of substitution, outlining the changes in mineral chemistry between the low- and high-grade biotites, have been recognised. These different types of substitution reflect the interrelated effects of grade, host-rock composition, and the structural and charge balance requirements of the biotite, which determine the composition of the biotite formed during metamorphism.

The decrease in Al content of the biotite with increasing grade in the greywackes is not characteristic of more-pelitic rocks. In pelitic rocks the biotite Al content remains constant with increasing grade, because it is buffered by the presence of Al-rich silicates besides feldspar (e.g. muscovite). However, these Al-rich silicates do not occur in the greywackes, and the Al content of biotite consequently decreases as phases requiring Al (commonly feldspar) form with increasing grade.

The Mn/Mn+Fe ratio of ilmenite is dependent on its paragenesis because of the different $K_{D(Mn)}$ values for ilmenite-chlorite, ilmenite-biotite and ilmenite-orthopyroxene.

P-T conditions are not well delineated, but pressures of approximately 1 kb are suggested, while temperatures appear to vary from 300-400^{o}C at the outer limit of the aureole to around 650^{o}C at the contact.